Modeling belowground water table fluctuations in the Everglades

Dario Pumo,[1,2] Stefania Tamea,[3] Leonardo Valerio Noto,[1] Fernando Miralles-Wilhem,[4] and Ignacio Rodriguez-Iturbe[2]

Received 17 November 2009; revised 7 September 2010; accepted 21 September 2010; published 25 November 2010.

[1] Humid lands, such as riparian zones, peatlands, and unsubmerged wetlands, are considered among the most biologically diverse of all ecosystems, providing a bountiful habitat for a large number of plant and animal species. In such ecosystems, the water table dynamics play a key role in major ecohydrological processes. The aim of the present study is to test with field data a recent analytical model for the estimation of the long-term probability distribution of the belowground water table position in groundwater-dependent environments. This model accounts for stochastic rainfall and processes such as infiltration, root water uptake, water flow from/to an external water body, and capillary fluxes. The water table model is tested using field data of groundwater levels recorded in three different sites within the Everglades (Florida, USA). A sensitivity analysis of the model to the soil and vegetation parameters is also carried out. After performing a procedure to determinate appropriate model parameters for the three sites, the steady state probability distribution functions of water table levels predicted by the model are compared to the empirical ones at both the annual and the seasonal time scale. The model is shown capable to reproduce many features of the observed distributions although there exist model predictions which still show some discrepancies with respect to the empirical observations. The potential causes for these discrepancies are also investigated and discussed.

Citation: Pumo, D., S. Tamea, L. V. Noto, F. Miralles-Wilhem, and I. Rodriguez-Iturbe (2010), Modeling belowground water table fluctuations in the Everglades, *Water Resour. Res.*, *46*, W11557, doi:10.1029/2009WR008911.

1. Introduction

[2] Wetlands are areas which are inundated or saturated by surface water or groundwater at a frequency and duration sufficient to support a prevalence of vegetations typically adapted for life in saturated soil conditions. They are characterized as having a water table that stands frequently at or near the land surface. Wetlands were initially considered marginal, and for this reason they have historically been victims of large-scale draining efforts, but they are indeed far more important in the biosphere than their limited worldwide spread (almost 7% of the world's ecosystems) would suggest [*Mitsch and Gosselink*, 2007]. Wetlands are dynamic, complex habitats, supporting high levels of biological diversity. Their natural ability to filter and clean water, contributes to the efforts to ameliorate the ever increasing challenge of decreasing water pollution. The importance of wetlands is also linked to their role in protecting coastlines from hurricanes and tsunamis, mitigating flooding of streams and rivers [*Costanza et al.*, 2008; *Srinivas and Nakagawa*, 2008]. In addition, wetlands provide an immense storage of carbon that, if released with climate shifts, could accelerate those changes. For all these reasons, the scientific community is currently devoting much attention to those crucially important ecosystems [e.g., *Novitzki*, 1979; *Gilvear et al.*, 1989; *Brinson*, 1993; *Ramsar Convention Bureau*, 1996; *Mitsch et al.*, 2009; *Eamus*, 2009].

[3] Wetlands are groundwater-dependent ecosystems (GDEs), namely, ecosystems whose current composition, structure and function are reliant on a supply of groundwater and that require access to groundwater to maintain their health and vigor.

[4] In GDEs soil-climate-vegetation mutual interactions control and at the same time are influenced by the water table depth and the soil water content. Water table fluctuations and soil moisture profiles in fact, play a fundamental role in major ecohydrologic processes, including infiltration, surface runoff, groundwater flow, land-atmosphere feedbacks, vegetation dynamics, nutrient cycling, and pollutant transport. The ecohydrological approach to the study of wetlands represents indeed a new frontier of scientific research presenting particularly challenging features because of the intermittency and uncertainty inherent to the rainfall regime, and as a consequence, the coupled stochastic dynamics of the soil moisture and the water table depth.

[5] In the recent past, such dynamics were mostly investigated either in terms of mean seasonal water fluxes (mean precipitation, evapotranspiration, drainage), or through more detailed numerical simulations of the soil water balance

[1]Dipartimento di Ingegneria Idraulica ed Applicazioni Ambientali, Università degli Studi di Palermo, Palermo, Italy.
[2]Department of Civil and Environmental Engineering, Princeton University, Princeton, New Jersey, USA.
[3]Dipartimento di Idraulica, Trasporti ed Infrastrutture Civili, Politecnico di Torino, Turin, Italy.
[4]Department of Civil and Environmental Engineering, Florida International University, Miami, Florida, USA.

0043-1397/10/2009WR008911

[e.g., *Feddes et al.*, 1988; *Berendrecht et al.*, 2004; *Yeh and Eltahir*, 2005]. *Salvucci and Entekhabi* [1994] studied the role of temporal variability, for different water table positions, on soil moisture time profiles via simulations based on the numerical integration of the governing equations in the unsaturated zone. Their simulations consisted of forcing the surface of a one-dimensional soil column, bounded at its base by a fixed water table, with the output of a stochastic event-based model of precipitation and potential evapotranspiration. In a different work, the same authors [*Salvucci and Entekhabi*, 1995] proposed a numerical method to determine the equilibrium water table position and the corresponding spatial structure of the mean recharge, discharge, evaporation, and surface runoff throughout a hillslope. *Bierkens* [1998] investigated the water table dynamics by means of a model that numerically solves a stochastic differential equation, assuming equilibrium soil moisture conditions; in this modeling stochasticity is introduced in the water balance as a generic noise term. *Kim et al.* [1999] proposed a transient, mixed analytical-numerical model to study the patterns of infiltration, evapotranspiration, recharge and lateral flow across hillslopes.

[6] Numerical calculations of soil moisture dynamics and their impact on vegetation are not always well suited for an effective analysis of the interdependence of soil, vegetation, and climate drivers, especially when it is necessary to account for the stochastic nature of these processes. Thus it is important to try to describe such interdependence, as much as possible, via analytical formulations.

[7] Most of the early analytical research in ecohydrology has concentrated on arid and semiarid ecosystems [e.g., *Porporato et al.*, 2001; *Rodriguez-Iturbe and Porporato*, 2004], where productivity strongly depends on soil water availability and the effect of water table dynamics on vegetation can be neglected; in such ecosystems, in fact, the water table, because of its deepness, can often be assumed mostly inaccessible to the same vegetation [*D'Odorico and Porporato*, 2006]. The search for analytical solutions [e.g., *Rodriguez-Iturbe et al.*, 1999; *Laio et al.*, 2001] of the stochastic soil water balance equation suggests the use of simple models of soil moisture dynamics, which are able to account for the random character of precipitation along with the pulsing character of soil moisture. *Rodriguez-Iturbe et al.* [2007] highlighted the need of an analytical framework for the study of the stochastic soil water balance in humid lands. Also, wetlands indeed can be considered water-limited environments, even if their dynamics are substantially different from those of arid and semiarid ecosystems [*Naiman et al.*, 2005; *Mitsch and Gosselink*, 2007]. In the case of wetlands, the hydrologic control on vegetation and microbial stress does not arise from water limitation but rather arises most frequently from waterlogging conditions and the consequent limitation on soil oxygen availability [e.g., *Kozlowski*, 1984; *Roy et al.*, 2000; *Brolsma and Bierkens*, 2007; *Bartholomeus et al.*, 2008]. At the same time plants may, in turn, affect the water table depth, as observed in several kinds of wetland [*Dacey and Howes*, 1984; *Dubé et al.*, 1995; *Roy et al.*, 2000; *Wright and Chambers*, 2002].

[8] *Ridolfi et al.* [2008] developed a probabilistic framework to investigate the coupled soil moisture–water table dynamics in the case of bare soil conditions. In two recent papers, *Laio et al.* [2009] and *Tamea et al.* [2009] proposed a process-based probabilistic model valid in the case of vegetated soils having roots interacting with saturated and unsaturated zones. Since this model, specific for GDEs characterized by belowground fluctuations of the water table position, has never been tested with real data, this paper aims to fill this gap. Confronting the model with data provides clues as to what processes may be missing from the conceptual model. Moreover, comparison with field results could provide important indications to improve the model in the future. The development of quantitative methods for the study of the stochastic water balance in wetland ecosystems could enable new and important research avenues in ecohydrology, for example providing a framework to understand the role of humid lands as filters for contaminated streams and aquifers and to investigate how hydrologic processes affect ecosystem productivity, the emergence of plant water stress, interspecies competition, the stability and resilience of wetland plant communities, and the complexity and nonlinearity of vegetation successional dynamics.

[9] In particular, the objective of this paper is to test the model by *Laio et al.* [2009], relative to the probabilistic study of water table fluctuations, through its application to different sites located in southeast Florida (USA) within the Everglades National Park. After a preliminary description of the model and the three sites chosen for its application, a sensitivity analysis of the model to the vegetation and soil parameters is performed. In particular, a Monte Carlo method has been used to study the effects of different soil parameters on the model outputs. Once appropriate model parameters have been fixed for each site, the model performances at both the annual and seasonal (two seasons: dry and wet) time scales are investigated, providing also possible causes for some discrepancies between the model predictions and the field observations.

2. Description of the Model and the Sites Considered

2.1. Analytical Modeling of Water Table Dynamics

[10] In this section, the basic concepts and assumptions of the analytical model are recalled, while for more detailed information, the reader is referred to the original papers by *Laio et al.* [2009] and *Tamea et al.* [2009].

2.1.1. Water Balance Equation

[11] The model developed by *Laio et al.* [2009] is founded on a simple process-based soil water balance equation forced by stochastic precipitation. The water balance accounts for rainfall infiltration, water table recharge, plant water uptake, capillary flux, groundwater flow, and coupling between water table fluctuations and soil moisture dynamics in the unsaturated portion of the soil column.

[12] Considering a positive upward vertical axis with origin at the soil surface, one can identify with $\tilde{y}(t)$ the depth of the water table, defined as the saturated surface at zero pressure head (Figure 1). The saturated capillary fringe is assumed to occupy a constant portion of soil above the water table, having a thickness equal to $|\psi_s|$, where ψ_s is the (negative) bubbling pressure head, or saturated matric potential. Thus the surface separating saturated and unsaturated soil lies at a depth $y(t)$ defined as

$$y(t) = \tilde{y}(t) - \psi_s, \tag{1}$$

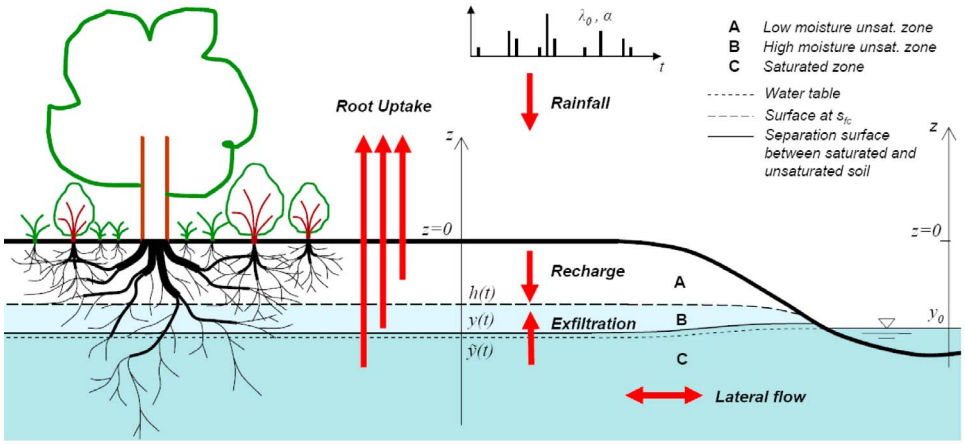

Figure 1. Schematic representation of the terms of the water balance equation and variables involved in the evaluation of the lateral flow [after *Laio et al.*, 2009].

[13] Since the model does not account for soil submergence and it is limited at $y \leq 0$, the shallowest water table position which can be captured lies at a depth ψ_s below the soil surface.

[14] The soil matric potential, $\psi(s)$, and the unsaturated hydraulic conductivity, $k(s)$, are related to the soil moisture, s, through the *Brooks and Corey* [1964] model truncated at small values of hydraulic conductivity (with $k(s) = 0$ for $s \leq s_{fc}$). The value of the field capacity, s_{fc}, is obtained by imposing $k(s_{fc}) = 0.05\ PET$, where PET is the potential evapotranspiration rate.

[15] Considering a homogeneous soil column at the plot scale (e.g., 100 m^2), the water balance equation with respect to the separation surface, y, can be written as

$$\beta(y) \cdot \frac{dy(t)}{dt} = Re(y,t) \pm f_l(y) - U_s(y) - Ex(y) \qquad (2)$$

where $\beta(y)$, $Re(y)$, $f_l(y)$, $U_s(y)$ and $Ex(y)$ are the specific yield, the recharge rate, the lateral flow from/to an external water body, the root uptake from the saturated zone and the exfiltration from the water table due to the capillary flux (Figure 1), respectively.

[16] Three different zones can be identified in the soil column: the saturated zone, the unsaturated zone with high moisture and the unsaturated zone with low moisture. At a certain time, t, the saturated zone (C in Figure 1) lies below the depth $z_{sup} = y(t)$, and has all the soil pores filled with water, i.e., soil moisture $s = 1$. The high-moisture unsaturated zone (HMUZ, B in Figure 1) has a soil moisture ranging from field capacity (s_{fc}) to saturation ($s = 1$) and, at a certain time t, is delimited by the depth $z_{inf} = y(t)$ and either the soil surface ($z_{sup} = 0$), if this is wetter than field capacity, or the depth $z_{sup} = h(t)$ (where $h(t)$ is the depth of the layer at field capacity at the time t), if the soil moisture content at the superficial layers is lower than s_{fc}. The low-moisture unsaturated zone (LMUZ, A in Figure 1) is present whenever the upper part of the soil column has a soil moisture below field capacity and, at a certain time t, it lies between the soil surface ($z_{sup} = 0$) and the depth $z_{inf} = h(t)$. The depth $h(t)$ depends on the steady state soil moisture profile and is a direct function of the water table position, as given by integration of the local soil water balance in the unsaturated soil (Richards equation). A stepwise function has been proposed by *Laio et al.* [2009] to approximate the relation $h(y)$, and the robustness of this approximation has been tested by the same authors for different soils and plant rooting depths through a comparison with the numerical solution.

[17] The model considers two different regimes: shallow water table (SWT) and deep water table (DWT). The critical depth y_c of the separation surface between the saturated and the unsaturated zone corresponding to $h(t) = 0$, marks the transition between these two regimes. The SWT regime is characterized by the absence of the LMUZ and occurs whenever $y(t) > y_c$; otherwise the regime is that of DWT. The critical depth y_c can be determined by integrating the Richards equation in steady conditions; since an analytical solution is not available, *Laio et al.* [2009] suggest the use of an approximate solution which is found to agree well with the solution obtained numerically for different types of soil and vegetation.

[18] The recharge rate term, $Re(t)$, represents the process of groundwater recharge, which is the result of rainfall infiltration and redistribution through the soil column. Rainfall at the daily level is the stochastic forcing of the dynamic system. Here, following previous studies [*Rodriguez-Iturbe et al.*, 1999; *Laio et al.*, 2006], the net rainfall reaching the soil after canopy interception is assumed to be well represented by a stationary marked Poisson process with rate λ_0. The marks correspond to independent and exponentially distributed daily rainfall depths with mean α. In SWT conditions, the rainfall frequency equals the recharge frequency with all the rainfall coming into the HMUZ contributing to recharge. The process of infiltration and water redistribution in the HMUZ are considered to occur instantaneously, at the daily time scale, because soil moisture values are larger than the field capacity [*Laio et al.*, 2006; *Botter et al.*, 2007]. In DWT conditions, not all the rainfall events reach the water table, and the LMUZ acts as a buffer which reduces the frequency of recharge events. The new frequency depends on the water table position, rainfall depth and the soil moisture content in the LMUZ. In fact, assuming that all rainfall events find the same average soil moisture content in the LMUZ, the sequence of the recharge events retains the Poissonian properties of rainfall occurrences [*Laio*, 2006] and the recharge rate will not depend on

the fluctuations of $s(z)$ but only on the local long-term average values. The recharge process has thus a mean depth α and a rate $\lambda(y)$ given by

$$\begin{cases} \lambda(y) = \lambda_0 & \longrightarrow SWT \\ \lambda(y) = \lambda_0 \cdot \exp\left[\dfrac{n \cdot h(y) \cdot \left[s_{fc} - \overline{s}'_m(h(y))\right]}{\alpha}\right] & \longrightarrow DWT \end{cases} \quad (3)$$

where λ_0 is the rate of net rainfall occurrences (e.g., after interception is accounted for), $h(y)$ is the depth of the boundary layer between the HMUZ and the LMUZ and $\overline{s}'_m(h)$ is the long-term average soil moisture in the LMUZ [*Tamea et al.*, 2009].

[19] The lateral flow f_l in equation (2) takes into account the presence of a nearby water body or a regional groundwater level, and it depends on the relative position of the local water table, $\tilde{y}$, and the free surface of the external water body. The external water body has a water surface at the depth y_0 (Figure 1), relative to the soil surface at the site under consideration, which is constant in time. The external water body is located at a distance from the site which is large enough to assume a horizontal water table at the site under analysis. The lateral flow can then be described by a linear relationship, similar to Darcy's law, for both the SWT and DWT conditions:

$$f_l(y) = k_l \cdot (y_0 - y - \psi_s) \quad (4)$$

where k_l is a constant of proportionality, whose estimation will be discussed in section 3.2.

[20] In the water balance equation the effect of evaporation, which is small compared to transpiration when a dense vegetation cover is present [*Laio et al.*, 2009], is neglected. The terms U_s and Ex in the water balance equation (equation (2)) represent the water losses from the saturated zone due to root uptake and capillary rise (exfiltration), respectively. The first term represents the effect of water uptake by roots allocated within the saturated zone while the second term is the upward vertical movement of water from saturated to partially saturated soil layers, due to capillary rise that, in turn, is driven by the difference in soil matric potential in the soil layers induced by plant water uptake, and thus dependent on the location and distribution of the roots.

[21] The model by *Laio et al.* [2009] considers three simplifying assumptions on the functioning of root uptake. The first assumption is that the uptake flux is unaffected by anoxic (saturated) conditions in the soil and, then, no uptake-reduction function is applied for large values of s. This assumption is justified by the fact that most of the plant species populating humid lands are well adapted to soil anoxic conditions and can cope with saturation conditions adopting different strategies to survive waterlogging. For example, they may develop anaerobic metabolisms and thus be able to increase oxygen provision to the roots [e.g., *Naumburg et al.*, 2005; *Vartapetian and Jackson*, 1997]. The second assumption is that a noncooperative root functioning system is considered neglecting compensation mechanisms [see, e.g., *Guswa*, 2005, 2008]. Thus, roots in each soil layer are considered to take up water independently of the others, without compensating for limitations in transpiration and uptake, which may occur somewhere along the soil profile. Finally, the third assumption is that the plot-scale averaged root distribution can be represented by a simple normalized function $r(z)$. Following other authors [e.g., *Schenk and Jackson*, 2002; *Schenk*, 2005], an exponential distribution of the root biomass, $r(z) = 1/b \cdot e^{z/b}$, is considered, where b is the average rooting depth. With these assumptions, the root uptake, $U(z)$, at the generic depth z, within the saturated zone, is directly proportional to the root density $r(z)$ and the maximum potential evapotranspiration rate, PET (which is controlled only by atmospheric conditions). Then, the total root uptake from the saturated zone (for both the cases of SWT and DWT) reads

$$U_s(y) = PET \cdot e^{\frac{y}{b}} \quad (5)$$

[22] The exfiltration term, Ex, takes into account the mechanism of capillarity due to vertical gradients of soil matric potential induced by plant transpiration. Following *Laio et al.* [2009], the term in the water balance equation for the cases of shallow and deep water table regimes, can be written as

$$\begin{cases} Ex(y) = PET \cdot \left(1 - e^{\frac{y}{b}}\right) & \longrightarrow SWT \\ Ex(y) = PET \cdot \left(e^{\frac{h}{b}} - e^{\frac{y}{b}}\right) & \longrightarrow DWT \end{cases} \quad (6)$$

[23] From equations (5) and (6), one can note that, under SWT conditions, the total flux from the saturated zone, leaving aside the lateral flux, (i.e., $U_s + Ex$), is constant and equal to the potential evapotranspiration rate. It is assumed that for $s < s_{fc}$, the hydraulic conductivity is null, then, the depth h (where $s = s_{fc}$) also represents the threshold above which the water table exerts no influence on the local soil water balance and, as a consequence, no capillary fluxes are present in the LMUZ.

[24] Finally, the specific yield, $\beta(y)$, in equation (2) converts the volumetric fluctuations (positive or negative) of water within the aquifer in the corresponding fluctuations in water table position. It depends on the water table depth and on the soil properties, as well as on the SWT or DWT condition. The specific yield was obtained by *Laio et al.* [2009]as

$$\begin{cases} \beta(y) = n - n\left[1 + \left(s_{fc}^{-\frac{1}{2m}} - 1\right) \cdot \left(\dfrac{y}{y_c}\right)\right]^{-2m} & \longrightarrow SWT \\ \beta(y) = n\left(1 - s_{fc}\right) + n \cdot \left(\dfrac{dh}{dy} - 1\right) \cdot \dfrac{1}{2m-1} \cdot \left(\dfrac{1 - s_{fc}}{1 - s_{fc}^{\frac{1}{2m}}} - 2ms_{fc} + s_{fc} - 1\right) & \longrightarrow DWT \end{cases} \quad (7)$$

where n is the porosity, m is the pore size index [*Brooks and Corey*, 1964], and dh/dy is the derivative of the $h(y)$ relationship given by *Laio et al.* [2009].

2.1.2. Probability Distribution of the Water Table Depth

[25] The model provides the stationary probability density function of the depth y of the surface marking the separation between saturated and unsaturated soil. It is possible to rewrite the soil water balance equation as

$$\frac{dy}{dt} = f(y) + g(y) \cdot \xi(y,t) \tag{8}$$

where the terms $f(y)$, $g(y)$ and $\xi(y)$ are

$$f(y) = \begin{cases} \dfrac{k_l(y_0 - y - \psi_s) - PET}{\beta(y)} & \longrightarrow SWT \\ \dfrac{k_l(y_0 - y - \psi_s) - PET \cdot e^{h(y)/b}}{\beta(y)} & \longrightarrow DWT \end{cases}$$

$$g(y) = \frac{1}{\beta(y)}$$

$$\xi(y,t) = \begin{cases} \mathrm{P}(\lambda_0, \alpha) & \longrightarrow SWT \\ \mathrm{P}\left(\lambda_0 \cdot \exp\left[\dfrac{n \cdot h(y) \cdot \left[s_{fc} - \bar{s}'_m(h(y))\right]}{\alpha}\right], \alpha\right) & \longrightarrow DWT \end{cases} \tag{9}$$

respectively.

[26] The above stepwise continuous first-order stochastic differential equation can be solved under steady state conditions. The solution for the case of a state-dependent noise rate $\lambda(y)$ is given by *D'Odorico and Porporato* [2004] and *Porporato and D'Odorico* [2004] as

$$p_Y(y) = \frac{C}{f(y) - \alpha\lambda(y)g(y)} \cdot \exp\left[-\int_0^y \frac{f(y)}{\alpha \cdot g(y) \cdot [f(y) - \alpha\lambda(y)g(y)]}\,du\right] \tag{10}$$

where C is a normalization constant obtained by setting $\int_{-\infty}^{0} p_Y(y) = 1$. The probability density function of the water table depth, $\tilde{y}$, is obtained with a simple translation, and reads: $p_{\tilde{y}}(\tilde{y}) = p_Y(y + \psi_s)$.

[27] The pdf of y (equation (10)) ranges from the soil surface, where the probability goes to zero, to the lower bound, $y_{\lim}$, representing the deepest position allowed by the model. This can be computed from the steady state water balance in the absence of rainfall [*Laio et al.*, 2009], i.e., $f_l(y_{\lim}) = U_s(y_{\lim}) + Ex(y_{\lim})$. As a consequence of these bounds, the pdf of the water table position ranges from ψ_s to $\tilde{y}_{\lim}$ (equal to $y_{\lim} + \psi_s$).

2.2. Description of the Sites

[28] The dense monitoring network covering the Everglades (Florida, USA) makes this areas an ideal location to test the model in virtue of the abundance of publicly available data sets (e.g., water table depths, rainfall, evapotranspiration, soil and vegetation properties, etc.) having long series of daily measurements. Some of the most important agencies monitoring the Florida Everglades together with their Web links, frequently referred to in this paper, include the following: U.S. Geological Survey (USGS, http://www.usgs.gov); Everglades Depth Estimation Network (EDEN; http://www.sofia.usgs.gov/eden); Florida Coastal Everglades-Long-term Ecological Research (FCE-LTER; http://www.fcelter.fiu.edu); South Florida Water Management District (SFWMD; http://www.sfwmd.gov).

[29] In particular, we choose three different sites where long historical series of daily data of groundwater depths, precipitation and evapotranspiration are available. Much of the Everglades landscape is subject to extended and prolonged flooding, especially during the wet season (from June to November). Since the model does not account for standing water, the sites have been chosen among those having water level fluctuations within the shallow soil layer in order to warrant that submergence of the sites is limited in time or not occurring. For this reason, the three sites chosen are only partially representative of the general conditions of water level fluctuations in the Everglades.

[30] All the sites are located in southeast Florida (USA), Dade County, within the Everglades National Park (Figure 2). Site 1 is located in the Florida Bay, very close to the sea. The gauging station is named Taylor River at Mouth (alias TS/Ph-7a), and the operating agency is the USGS. The data of groundwater levels, rainfall and potential evapotranspiration are available at the EDEN, USGS and FCE-LTER Web sites. The site, located within the Taylor Slough watershed, presents flat topography, with a tidal creek and limestone bedrock. The shallowest portion of soil is made up of wetland peat (>1 m thick) while the vegetation is mangrove.

[31] Site 2 is located within the so-called Frog Pond Area, between the canal C111 and the levee L31W. The groundwater well, identified by the code FRGPD2, is operated by SFWMD, and the data are available at their Web site. For precipitation and evapotranspiration data, the station considered is the L31W (alias TS/Ph-1b), managed by ENP (Everglades National Park), with data available at the EDEN Web site. This weather station is almost 2 km from the groundwater well FRGPD2. This site is also located within the Taylor Slough watershed, and is characterized by flat topography and limestone bedrock. The shallower soil is wetland marl and the vegetation is mainly sparse sawgrass.

[32] Site 3 is located near the levee L31W, close to the northern area of the Taylor Slough. The groundwater well is R158G and the operating agency is the ENP. Groundwater data are available at the SFWMD Web site. For precipitation and evapotranspiration data, the station considered is TS2 (alias TS/Ph-2), managed by ENP, with data available at the EDEN Web site; this station is located about 2 km from the station R158G. The topography of the area is flat and the geology is characterized by limestone bedrock. The soil presents a layer of wetland marly peat (about 1 m thick) and the vegetation cover is sparse sawgrass.

[33] In the evaluation of the lateral flow contribution, it is important to point out that for Site 1, the closest external water body is the ocean, while for the other two sites the closer external water bodies are large canals (C111 and L31W), where daily records of water levels are also available. These canals are part of the water management system developed in the South Florida throughout most of the 20th century. The canals were initially conceived as drainage canals, with small success for their original purpose. The initial impact of the canal network on the Everglades groundwater was that of lowering the water table thus creating a hydraulic gradient between the Everglades and the

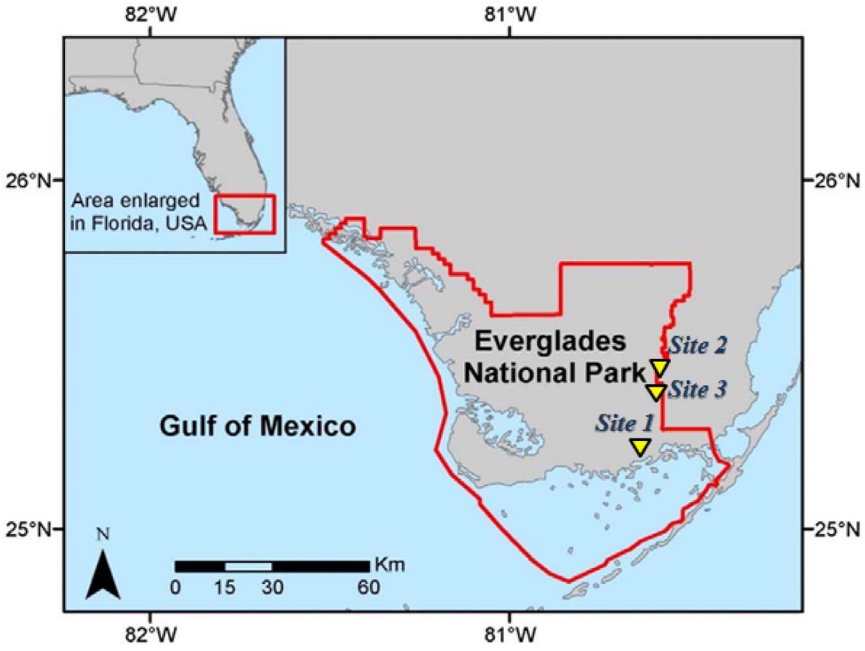

Figure 2. Locations of the three sites used for the application of the model.

Atlantic Ocean that caused an unexpected increase of marine intrusion. For this reason, the most recent engineering works have been addressed toward the reestablishment of the natural conditions of the water levels within the Everglades. Canals and levees construction expanded greatly during the 1950s and 1960s, reaching its final phase in the 1980s, with the completion of the Everglades-South Dade conveyance system [*Renken et al.*, 2005].

2.3. Analysis of the Historical Data Series of Water Table

[34] The ground elevation for each site has been derived from the National Map Seamless Server provided by the USGS, having a resolution of approximately 30 m. The horizontal datum is the NAD83 (North American Datum of 1983) while the vertical datum is the NAVD88 (North American Vertical Datum of 1988). The ground elevations found at the three sites are shown in Table 1.

[35] Table 1 gives for each site the observation period, the mean annual groundwater depths below the soil surface, as well as the mean seasonal water table positions during the wet and dry season. Figure 3 shows the time series of water table depths measured in cm and referred to the NAVD88; the original data for Sites 2 and 3 were referred to the NGVD29 (North American Geodetic Datum of 1929), thus they have been converted to the NAVD88 with the vertical conversion factors provided by the EDEN Web site for the nearby stations L31W (Site 2) and TS2 (Site 3). The three time series clearly show strong seasonality, mainly driven by rainfall: the water table is shallower during the wet season (from June to November) when most of the precipitation occurs, while it lies in deeper layers during the rest of the year. The behavior of groundwater fluctuations in Figures 3a, 3b, and 3c, also shows the presence of some periods of inundation which are relatively short and not very numerous, and thus not crucial for the purposes of this paper.

[36] Figure 4a (left), Figure 4b (left), and Figure 4c (left) show the autocorrelation functions (ACF) of the historical water table data relative to the three sites. The ACFs highlight the strong seasonality of the water level time series with a period of 365 days. The seasonality has been removed from each series by subtracting the mean daily groundwater level throughout the years from each daily value. This procedure allows one to obtain the time series of water table fluctuations around the mean value (referred to

Table 1. Information About the Groundwater Measurements at the Three Sites[a]

	Site 1	Site 2	Site 3
Ground elevation (m a.s.l.) (NAVD88)	0.10	1.09	0.83
Water table measurement station	TS/Ph7a	FRGPD2	R158G
Operating agency	USGS	SFWMD	ENP
Water table observation period	2 Oct 1995 to 26 Jan 2009	11 Oct 1996 to 14 Jan 2009	1 Oct 1983 to 3 Nov 2003
Mean water table depth (annual) (cm)	−30.3	−44.6	−52.1
Standard deviation (annual) (cm)	8.7	18.2	19.5
Mean water table depth (dry season) (cm)	−34.6	−54.8	−61.3
Standard deviation (dry season) (cm)	7.9	16.2	18.5
Mean water table depth (wet season) (cm)	−25.4	−34.1	−41.0
Standard deviation (wet season) (cm)	6.9	13.7	14.3

[a]Ground elevations in meters above the sea level (NAVD88). Dry season from December to May; wet season from June to November. Measurements in cm below the soil surface.

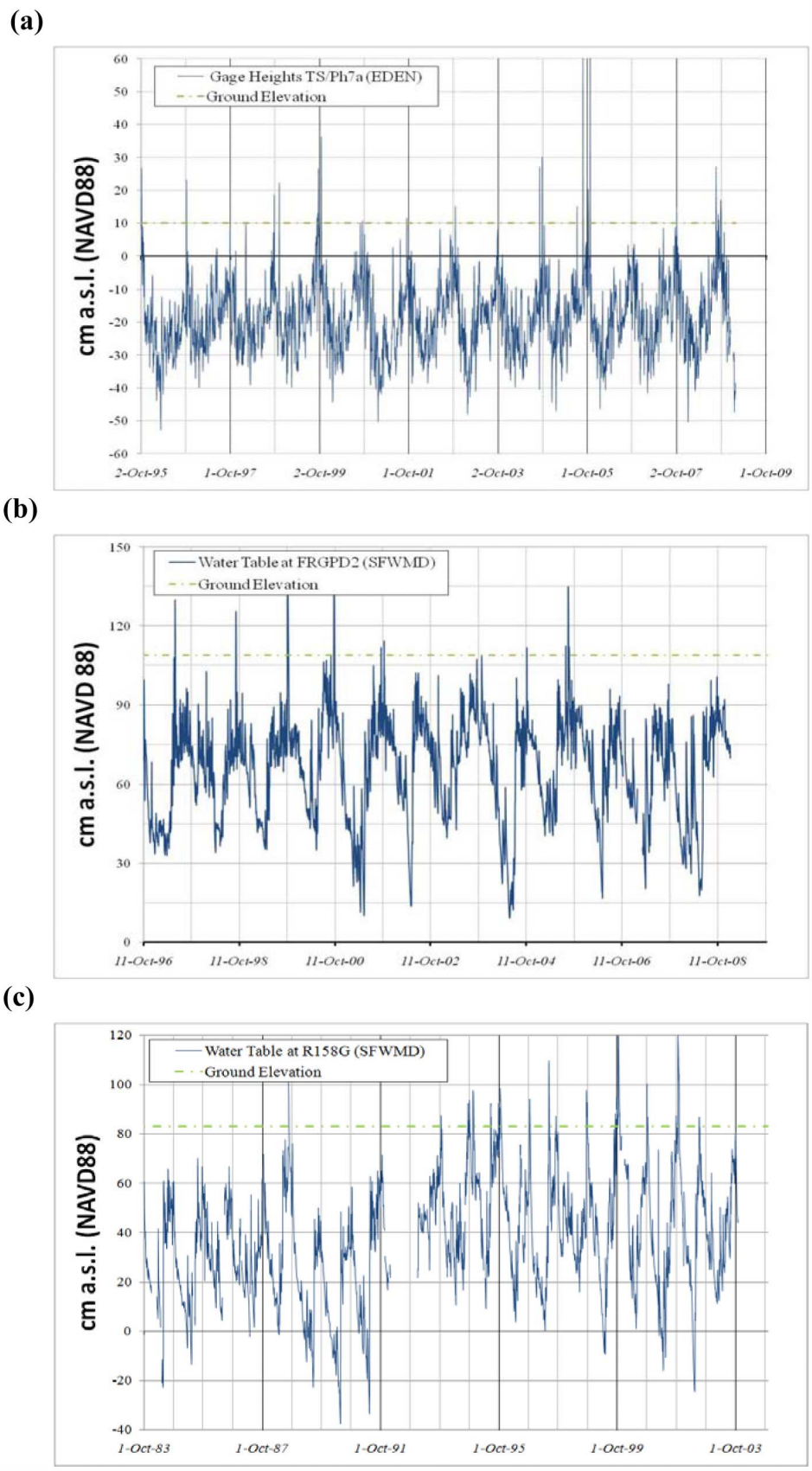

Figure 3. Time series of water table levels and ground elevation for (a) Site 1, (b) Site 2, and (c) Site 3. Elevations are in centimeters above the North America Vertical Datum 1988.

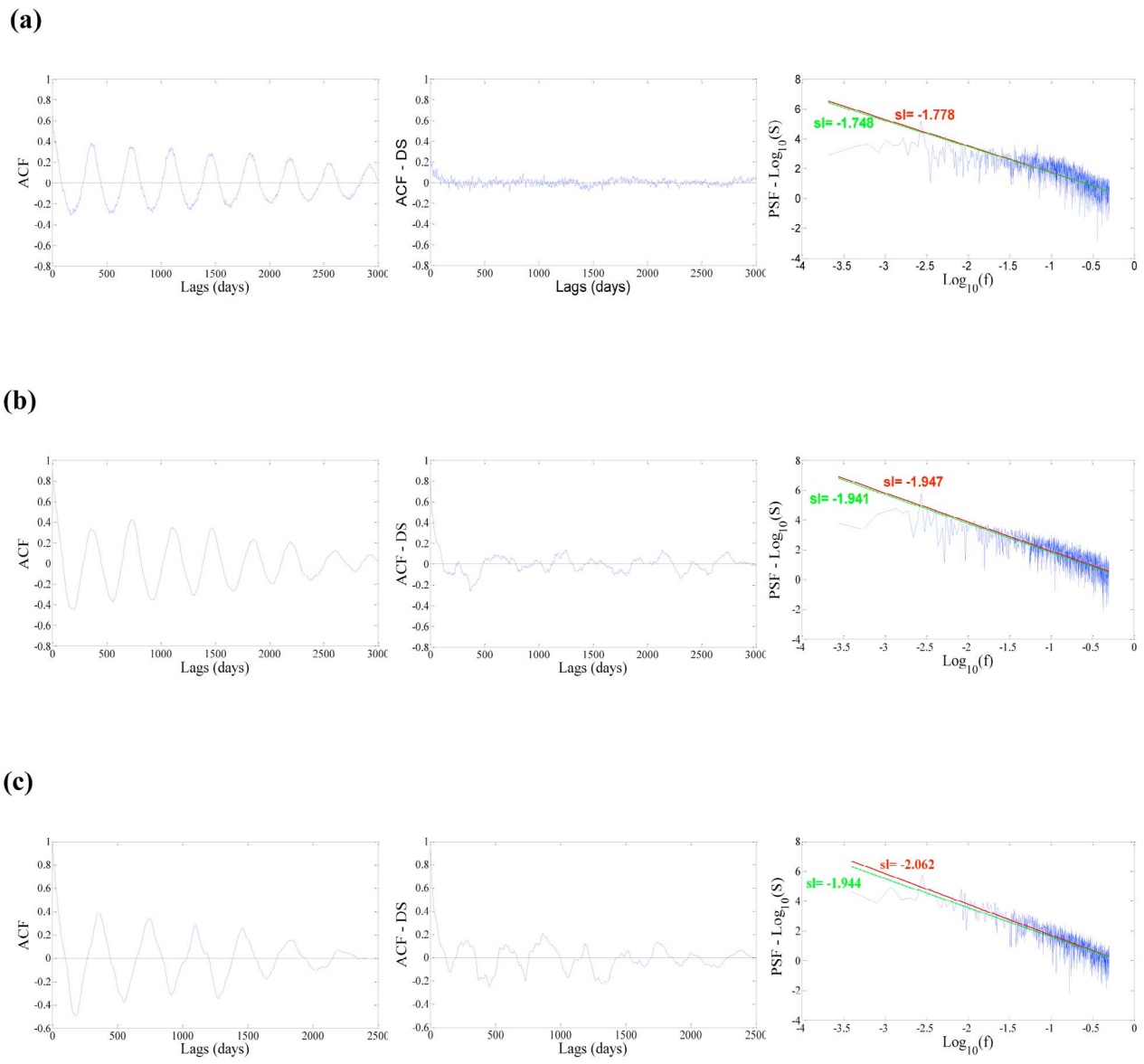

Figure 4. (a) Site 1, (b) Site 2, and (c) Site 3. Autocorrelation function (ACF) for (left) the original water table series and (middle) for the detrended series after the removal of the seasonal cycle (ACF – DS). (right) The power spectra functions (PSF) for the original series, with the slopes marked in red. The slopes in green refer to the detrended series.

here as detrended series) whose ACFs (Figure 4a, middle; Figure 4b, middle, Figure 4c, middle) show less relevant peaks without strong periodicity. One can notice that the detrended ACF for Site 1 (Figure 4a) is rather different from those of the other sites (Figures 4b and 4c) with Sites 2 and 3 maintaining higher correlation values in the detrended series. This could be due to the different nature of the influence of the external water body on the dynamics of the water levels; as mentioned above, in the case of Site 1 the closest water body is the ocean while the other two sites are controlled by canals. The seasonal component of the ocean influence is more regular and thus more effectively removed after detrending procedure. The presence of high correlation values in the detrended series for Sites 2 and 3 may in fact result from the human management of the nearby canals.

[37] The Power Spectra Functions (PSF) of the original data in the three case studies are shown in Figure 4a (right), Figure 4b (right), and Figure 4c (right), which also show their slopes (*sl*), in double logarithmic graphs, evaluated via least squares applied to the highest frequencies. The slopes corresponding to the detrended series are also given and, as expected, are very similar to the original ones. One can notice that the largest value of the PSFs occurs at frequency of $10^{-2.56}$, corresponding to the annual cycle (e.g., 1/365 days^{-1}).

3. Estimation of the Model Input Parameters

[38] The average annual rainfall in South Florida varies from 120 to 160 cm, depending upon location [*Lodge*,

Table 2. Mean Annual and Seasonal Values of the Rainfall Parameters Depth α, Frequency λ, and Total Precipitation Amount Θ and Potential Evapotranspiration (PET)[a]

Site	Weather Station Associated (EDEN)	Rainfall			PET	Rainfall			PET	Rainfall			PET
		α (cm)	λ (1/d)	Θ (cm/yr)	(cm/d)	α (cm)	λ (1/d)	Θ (cm/yr)	(cm/d)	α (cm)	λ (1/d)	Θ (cm/yr)	(cm/d)
1	Taylor River at Mouth	0.79	0.347	99	0.42	0.62	0.206	23	0.37	0.86	0.491	77	0.46
2	L31W	0.82	0.431	130	0.38	0.71	0.245	32	0.34	0.87	0.621	99	0.42
3	TS2	0.79	0.414	119	0.39	0.70	0.244	31	0.35	0.83	0.588	89	0.43

[a]Dry season from December to May; wet season from June to November. The weather stations are managed by SFWMD, and the data are available at the EDEN Web site (http://www.sofia.usgs.gov/eden).

2004]. In an average year, about 60% of the rainfall falls in the 4 month summer period of June through September, and only 25% falls in the 6 month dry season from November through April. May and October are pivotal months with inconsistent rainfall. According to FCE-LTER the local climate at the three sites chosen is subtropical moist with distinctive wet (June–November) and dry (December–May) seasons. In this study, two different parametric aggregation schemes are investigated: annual and seasonal. In the annual analysis the model uses as input parameters the average annual values for the potential evapotranspiration, for the rainfall parameters (mean depth and frequency) and for the elevation of the water surface in the nearest external water body. In the seasonal analysis, following the FCE-LTER subdivision of the hydrological year, the model considers two different seasons, each one having its own set of input parameters: dry season (from December to May) and wet season (from June to November). The two different schematizations (annual and seasonal) consider the same soil and vegetation parameters (time invariant quantities).

3.1. Rainfall and Evapotranspiration

[39] The climatic forcings that the water balance model requires are the daily potential evapotranspiration rate and the two rainfall parameters: daily mean depth α and interarrival rate λ. The EDEN Web site provides historical series of rainfall and potential evapotranspiration useful for the generation of such climatic parameters.

[40] Rainfall data based on Next Generation Radar (NEXRAD) provide a complete spatial coverage of rainfall amounts for the State of Florida. The NEXRAD coverage for the South Florida Water Management District area includes rainfall amounts at 15 min resolution intervals for the period 1 January 2002 to present with a spatial resolution of 2 km (EDEN Web site). The daily rainfall series considered for the three sites cover the period from 01/01/2002 to 09/30/2008. The annual and seasonal values of α and λ obtained from the series in the three different sites are summarized in Table 2.

[41] Daily potential evapotranspiration (PET) estimates on a 2 km resolution grid have been produced by EDEN for the State of Florida by means of a model that uses solar radiation obtained from Geostationary Operational Environmental Satellites (GOES) and climate data coming from the Florida Automated Weather Network, the State of Florida Water Management Districts and the National Oceanographic and Atmospheric Administration (NOAA). Daily PET values (in millimeters) are then extrapolated by location for each of the EDEN stations and published at the EDEN Web site. The daily series of potential evapotranspiration considered in this work for the three sites are from 06/01/1995 to 12/30/2007. Table 2 shows the mean daily values of potential evapotranspiration during the year and during the two seasons, for each site.

[42] From Table 2 it is possible to note that, for the considered sites, about 75% of the average annual precipitation is concentrated during the wet season, when the average values of potential evapotranspiration are about 24% higher than in the dry season.

3.2. Parameters for the Lateral Flow Evaluation

[43] The lateral flow term (equation (4)) requires two parameters to be estimated: y_0 and k_l. The model parameter y_0 corresponds to the depth of the free surface in the nearest water body from the site, measured with respect to the soil surface at the same site, and it is assumed to be constant in time, while k_l is the proportionally constant for the saturated lateral flow.

[44] In the case of Site 1, the external water body is the ocean (with a distance from the site of almost 70 m) and y_0 corresponds to the opposite of the ground elevation at the site (same absolute value but opposite sign). For Sites 2 and 3 the nearest water bodies are two different water canals with available measurements of daily water levels. The reference elevations y_0 are taken as constant and equal to the mean annual value for the annual analysis and to the mean seasonal values for the seasonal analysis. At Site 2, the nearest water body is canal C111 (with a distance from the site of near 410 m), whose historical daily series of water levels recorded at station S176H has been used. For Site 3 the nearest canal is levee L31W (almost 370 m from the site), with a gauging station (S175H) about 2 km from the groundwater well. The observation periods, the mean annual and seasonal values of the water levels in the canals, the ground elevations and the resulting annual and seasonal values of y_0 for both sites are summarized in Table 3.

[45] The model parameter, k_l, can be evaluated by means of an inverse procedure involving the time series of measurements of the water table depths. With a long series representative of the long-term behavior of the water table fluctuations, one can assume the value of $\tilde{y}_{\lim}$ (i.e., the deepest position allowed by the model; see section 2.1.2) as being equal to the deepest position of the water table recorded during the observation period, $\tilde{y}_{\min}$, corresponding to the position of the water table after the longest dry period (in absence of rainfall). The value of k_l can then be computed from the steady state water balance in the absence of rainfall (i.e., $f_l(y_{\min}) = U_s(y_{\min}) + Ex(y_{\min})$), by using equations (4),

Table 3. Mean Annual and Seasonal Water Levels in the C111 and L31W Canals and Annual and Seasonal Values of the Model Parameter y_0 for Sites 2 and 3[a]

	Site 2	Site 3
Water canal	C111	L31W
Water level measurement station	S176H	S175H
Operating agency	SFWMD	SFWMD
Water level observation period	1 Jan 1978 to 30 Jun 2007	17 Jun 1970 to 8 Jul 1997
Water levels (m a.s.l.) (NAVD88)		
Annual	0.83	0.56
Wet season	0.91	0.73
Dry season	0.75	0.37
y_0 (m)		
Annual	−0.26	−0.27
Wet season	−0.18	−0.08
Dry season	−0.36	−0.46

[a]The y_0 values are in meters below the soil surface for each site. For Site 1, the nearest water body is the ocean, and y_0 is simply the opposite of the ground elevation (−0.10 m). Dry season from December to May; wet season from June to November.

(5) and (6) with $y = y_{min}$. It is important to point out that his procedure requires the preliminary computation of the soil and vegetation parameters and thus the obtained values of k_l are related to the evaluation of these parameters.

3.3. Vegetation Parameters

[46] The dominant vegetation within the Everglades is constituted by sawgrass, specifically called Jamaica swamp sawgrass, although many other marsh plants are also present in the region [*Lodge*, 2004]. In the sites under study, the vegetation is mainly made up by mangrove at Site 1 and by sparse sawgrass at Sites 2 and 3 (FCE-LTER). Sawgrass vegetation in the Florida Everglades includes species such as *Claudium jamaicense*, *Eleocharis cellulose, E. elongata*, *E. interstincta* and *Panicum hemitomon*. Sawgrass is a coarse, rhizomatous, perennial sedge. Often it grows in dense, nearly monospecific stands which result from an extensive network of rhizomes. Apical meristems arise from the top of the rhizomes. In the Everglades, *Yates* [1974] found that rhizomes were generally within the top 10 cm in marl soil, and within the top 15–20 cm in peat.

[47] Mangrove vegetation in South Florida includes species such as *Rhizophora mangle*, *Avicenna germinas*, *Laguncularia racemosa* and *Conocarpus erectus*. Some of the main features and botanical characteristics of this species are provided by *Little* [1983] and the U.S. Forest Service Web site (http://www.fs.fed.us). Mangrove is usually an evergreen shrub 1.5 to 4 m tall which sometimes can also be present as a tree (for species such as *Avicenna germinas* and *Lagunaria racemosa*) with heights up to 12 m (vegetation at Site 1 is classified as mangrove with low stature). The root system consists mainly of laterals and fine roots that are dark brown, weak and brittle, and have a corky bark (*Conocarpus erectus*). Mangroves are an example of salt-resistant halophyte which have special features (adaptations) allowing them to cope with their difficult environment. The three main ways that mangroves deal with the problem of too much salt are the following: (1) by eliminating it through special salt-secreting glands in their leaves, (2) by storing it in leaves and stems that are shed at the end of the growing season, and (3) by keeping it from entering their cells by means of special membranes in their roots. This fact explains the presence of this kind of vegetation in tidal areas, as in the case of Site 1, and justifies the lack of consideration of salt effects in the model being used.

[48] The model by *Laio et al.* [2009] assumes an exponential distribution of the roots into the soil. Using the information available on the vegetation cover of the three sites, the parameter b (average rooting depth, equation (5)) has been assumed equal to 12 cm for the mangrove vegetation (Site 1) and 10 cm for the sawgrass (Sites 2 and 3). This assumption is not critical since, as it will be shown in section 4.1, the influence of the average rooting depth on the general behavior of the pdf's of water table depth is weak in the cases studied here. With these parameters, the model considers the root biomass concentrated mainly within the top 17–20 cm of the soil (about 80% of the total root biomass), while only 5% of the total biomass is deeper than 31–37 cm (with the lower values referring to sawgrass while the higher ones to mangrove).

3.4. Soil Parameters

[49] In this section some soil properties at the three sites are discussed with the aim of finding appropriate ranges for the model parameters. These will then be used in the sensitivity analysis of the model results, which will be presented in section 4.

[50] Two soil types are usually present in the Florida Everglades: marl and peat. Marl is the main soil of the short-hydroperiod wet prairies near the edges of the southern Everglades while peat is more common in Everglades marshes (Everglades peat and Loxahatchee peat). In particular, Everglades peat is made up almost entirely of the remains of sawgrass [*Lodge*, 2004].

[51] The existing body of knowledge concerning peat soil is not as large as that concerning mineral soil. However, in recent years, there has been increasing interest about wetlands [*Hoag and Price*, 1995] which encouraged an increasing number of analysis focused on the hydraulic properties of peat [*Boelter*, 1965; *Ingram*, 1967; *Hoag and Price*, 1995; *Holden and Burt*, 2003; *Rizzuti et al.*, 2004; *Rosa and Larocque*, 2008]. Almost all the studies agree in the fact that the characteristics of peat strongly depend on the nature of peat, in terms of organic matter fraction and botanical composition.

[52] Peat must contain no more than a certain amount of inorganic content (20% is a typical value [see *Myers*, 1999]). The ash content (or mineral content) for the Everglades soils usually ranges from about 25% to 90%; however, despite this high percentage of mineral content, it behaves hydrologically as peat [*Myers*, 1999]. Porosity in pure peat is high if compared to that of mineral soils. As the percentage of peat in a mixture peat-mineral soil increases from zero to 100%, the porosity increases from 40% to 90% [*Boggie*, 1970; *Myers*, 1999; *Walczak et al.*, 2002].

[53] A generic soil classification at the three sites under analysis is given by the FCE-LTER Web site. The soil at Site 1 is classified as wetland peat, at Site 2 the soil is wetland marl, and at Site 3 is wetland marly peat. The FCE-LTER Web site provides also the fraction of organic matter in the three sites: 22% (Site 1); 14% (Site 2); 25% (Site 3). Thus, according to the relation porosity-peat fraction presented by *Myers* [1999], the porosity in the three sites

should vary within the range from 0.45 to 0.53 (Site 3). For the sensitivity analysis of the model to the soil parameters that will be discussed in section 4, a slightly wider range of porosity, n, is investigated taking into account values from 0.40 to 0.55.

[54] Many researchers [e.g., *Boelter*, 1965; *Ingram*, 1967; *Sturges*, 1968; *Dai and Sparling*, 1973; *O'Brien*, 1977; *Chason and Siegel*, 1986] have attempted to measure the saturated hydraulic conductivity of wetland soils using traditional methods and found values ranging from 10^{-1} to 10^{-7} cm/s, with most of the values falling between 10^{-3} and 10^{-5} cm/s (i.e., from 1 to 85 cm/d). After a series of tests on undisturbed soil samples within southern Florida, *Myers* [1999] found values of the saturated hydraulic conductivity ranging from 0.63 to 25.92 cm/d. These values are also quite close to those obtained for peat samples by other authors from laboratory analysis [*Naasz et al.*, 2005; *Katimon and Melling*, 2007]. From these considerations, for the sensitivity analysis the parameter k_s (i.e., saturated hydraulic conductivity) has been assumed potentially ranging from 0.5 to 40 cm/d.

[55] It is important to point out that the model developed by *Laio et al.* [2009] assumes the soil column to be homogeneous and isotropic. Actually, the pure peat porosity decreases as the depth increases reaching an almost constant value in the catotelm zone (deeper layer with a well-decomposed peat) while the hydraulic conductivity of the acrotelm (shallower layer commonly between 0 and 20 cm and made up of undecomposed dead plant material) has been found to be up to five orders of magnitude greater than that of the catotelm [*Boelter*, 1965]. Moreover, pure peat presents a strong anisotropy in hydraulic conductivity with horizontal conductivity usually greater than the vertical one [*Weaver and Speir*, 1960; *Boelter*, 1965]. This anisotropy can be observed also in the vertical direction: when the flux of water is upward, the peat can present a slightly higher saturated conductivity than when it is downward oriented [*Myers*, 1999]. Although the two assumptions of homogeneity and isotropy may appear too severe if applied to a pure peat, they can be adopted if the ash content is as elevated as in the sites under consideration and the soil is a mixture peat/mineral soil with a small fraction of organic soil.

[56] The scarcity of information in literature about Brooks and Corey model parameters specific for peat and marly soils and the extreme variability of these among different types of organic soils, leads us to consider a wide range of variation for the pore size distribution index, m, and the bubbling pressure head, ψ_s. In particular, in the sensitivity analysis of the model to the soil parameters, a range from 0.08 to 0.30 has been considered for m, while a range from −2 to −30 cm has been considered for ψ_s, in the attempt to cover all the potential values relative to the three different sites. Some recent research confirms the analogy between organic and clayey soils; for example, *Myers* [1999] investigating peat characteristics within the Florida Everglades, states that organic matter in these soils, as well as clayey soils, is known to interact with water at a microscopic level through chemical and electrostatic forces. Moreover, as in clays, shrinking and swelling behavior in organic soils may show hysteretic behavior. The values of porosity for the three sites derived from the relation porosity-peat fraction by *Myers* [1999] are rather similar to those typical of silty clay and clay loam [*Rawls and Brakensiek*, 1989]. The pore size distribution index, m, for silty clay and clay loam, according to *Rawls and Brakensiek* [1989], is equal to 0.127 and 0.194, respectively, that are then the values that one could expect in the three sites under analysis, considering the analogy between clayey and organic soils. According to the water retention curves found by *Myers* [1999] for some isolated wetlands of southern Florida, the bubbling pressure head should be in the order of about −10 cm. *Naasz et al.* [2005] analyzed a peat by means of laboratory experiments (using the Instantaneous Profile Method) during a wetting-drying cycle. The same authors provide two pairs of parameters for the van Genuchten retention model; one is relative to the wetting values while the other refers to the drying ones. Assuming an average behavior, and thus using mean parameter values between the two different pairs provided by *Naasz et al.* [2005], the value of bubbling pressure head, ψ_s, obtained after a procedure to convert van Genuchten model parameters into Brooks and Corey model parameters [*Morel-Seytoux et al.*, 1996], results equal to −9.19 cm, a value very close to that obtained by *Myers* [1999].

4. Analysis and Results

[57] The comparison between the model results and the observed water table levels has been carried out in terms of pdf's of the water table depth as well as through the autocorrelation and power spectrum functions.

[58] The model does not account for water levels above the soil surface and describes fluctuations of the saturated zone up to the soil surface which corresponds to finding the water table at a depth $\tilde{y} = \psi_s$. This is thus taken as the upper threshold value (see section 2.1.1). The rare and short periods of submergence occurring at the considered sites are limited to a few days per year, and have been ignored in the analysis. Only the water table positions below the depth ψ_s have been then considered in the computation of the empirical distribution functions.

[59] The annual analysis has been carried out with a set of model input variables (rainfall parameters, potential evapotranspiration, water levels into the canals) evaluated as annual average values from the daily time series. The measured time series are simultaneous only for a relatively short period of time and do not cover the whole time span of the water level measurements. However, since the aim of this work is to characterize the long-term hydrological behavior of the water table at the different sites, the entire series of water level data has been used in the analysis. The seasonal analysis has been carried out by splitting the annual time series into two seasons (i.e., computing the average seasonal values for the daily depth of rainy days, the rate of rainy day occurrences, the potential evapotranspiration and the water surface position of the external water bodies). The resulting seasonal model pdf's are then compared with the distributions of the observed water table depth for each season (i.e., seasonal empirical pdf's).

4.1. Parameter Estimations and Model Sensitivity Analysis

[60] In order to perform a sensitivity analysis of the model to the soil and vegetation parameters, the rainfall and evapotranspiration parameters reported in section 3.1 (Table 2)

Table 4. Vegetation Parameters and Best Combinations of Soil Parameters m, k_s, n, and ψ_s for Sites 1, 2, and 3

	Site 1	Site 2	Site 3
Vegetation type	mangrove	sawgrass	sawgrass
Average rooting depth, b (cm)	12	10	10
Soil type	peat	marl	marly peat
Pore size dist. index, m	0.154	0.126	0.188
Sat. hydr. conduc., k_s (cm/d)	13.16	34.17	32.87
Porosity, n	0.514	0.542	0.518
Bubbl. pres. head, ψ_s (cm)	−12.46	−11.52	−17.21

and the values of y_0 in Table 3 (see section 3.2) are fixed for each site.

[61] The sensitivity analysis of the model to the model vegetation parameter shows that the influence of b on the general behavior of the model pdf's of water table depth is rather weak and it decreases as the saturated hydraulic conductivity increases, while it is practically constant as the other soil parameters (i.e., porosity, pore size distribution, bubbling pressure head) change. For k_s within the range of potentially suitable values for the considered sites (i.e., k_s = 10–35 cm/d, as it will be shown below), b has only a marginal impact on the model pdf of water table depth, with pdf's very similar with each other for b ranging from 1 to 15 cm and only slightly shifted toward deeper positions of the water table for b ranging from 15 to a very high value such as 100 cm.

[62] The sensitivity analysis of the model to the soil parameters is performed using a Monte Carlo method through the consideration of many different combinations of the four soil parameters (i.e., n, k_s, m and ψ_s), each one randomly chosen within the ranges pointed out in section 3.4. For each of these combinations, the parameter k_1 is obtained through the procedure described in section 3.2. The vegetation parameters used here are those described in section 3.3 (Table 4).

[63] Each simulation, relative to a set of soil parameters, yields a pdf of the water table depth whose values of mean (μ^{mod}), median (md^{mod}), standard deviation (σ^{mod}), and skewness (γ_1^{mod}), are also computed. These statistics are then compared to those computed from the empirical pdf (i.e., μ^{obs}, md^{obs}, σ^{obs}, γ_1^{obs}) obtaining the values of $\Delta\mu$ ($|\mu^{mod} - \mu^{obs}|$), Δmd ($|md^{mod} - md^{obs}|$), $\Delta\sigma$ ($|\sigma^{mod} - \sigma^{obs}|$) and $\Delta\gamma_1$ ($|\gamma_1^{mod} - \gamma_1^{obs}|$).

[64] An example of the results of the sensitivity analysis is shown in Figure 5; the four plots report the values of $\Delta\mu$, Δmd, $\Delta\sigma$, and $\Delta\gamma_1$ (computed at the annual scale) as a function of ψ_s. The lowest deviations of all the model statistics from the empirical ones are obtained with combinations of soil parameters having values of ψ_s ranging from −8 to −15 cm. In particular, the differences between the skewness coefficients are strongly correlated to ψ_s, showing an almost linear behavior with decreasing values of $\Delta\gamma_1$ as ψ_s increases.

[65] Moreover the sensitivity analysis shows that the model results are more sensitive to k_s and ψ_s than to n and m, especially with regards to the seasonal parameterization. Analyzing the relations of $\Delta\mu$ as a function of the four soil parameters, one can notice that most of the combinations of soil parameters with low values of $\Delta\mu$ are characterized by values of ψ_s and k_s concentrated in quite narrow ranges while the corresponding ranges of n and m are rather wide.

[66] Similar considerations can be made by observing Figure 6 that shows the model pdf's of water table depth obtained for Site 3, changing one soil parameter at a time and keeping the other three unchanged. In particular, five different values chosen within the ranges provided in section 3.4 are analyzed for each parameter. Once again the model is more sensitive to k_s and ψ_s than it is to n and m. Despite the wide ranges chosen, the model pdf's obtained by using different values of n and m, maintain similar central location, dispersion and shape. When varying k_s it can be noticed that the different pdf's obtained for k_s < 30 cm/d are rather different with each other, while they are rather similar for higher values of the saturated hydraulic conductivity. This is a consequence of the fact that for relatively low

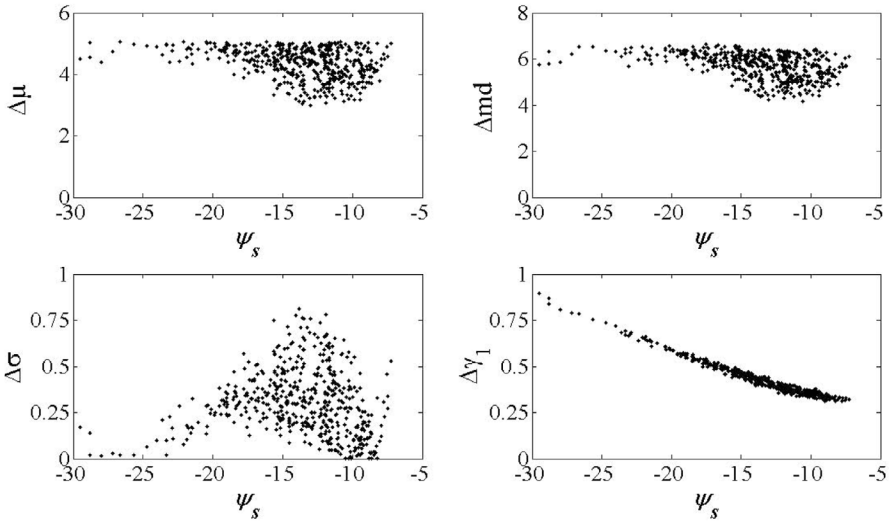

Figure 5. Values of the differences between the statistics derived from the annual model pdf's of water table depth and the annual empirical pdf as a function of ψ_s (cm): (top left) $\Delta\mu$ (cm), (top right) Δmd (cm), (bottom right) $\Delta\gamma_1$, and (bottom left) $\Delta\sigma$ (cm). Only 500 combinations of the soil parameters for Site 1 are shown.

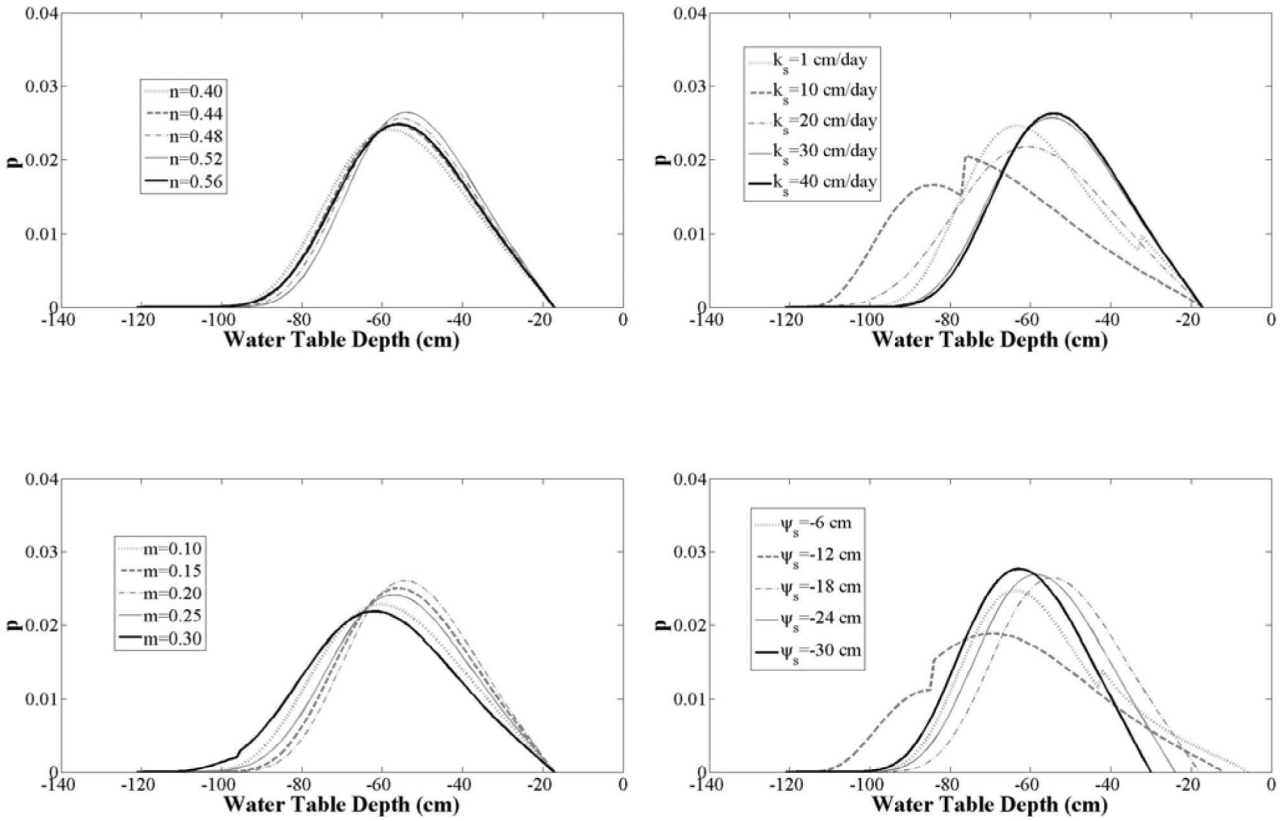

Figure 6. Sensitivity of the model to the four soil parameters for Site 3. (top left) n ranging from 0.40 to 0.56, other model parameters corresponding to those of the best combination for Site 3 (Table 4). (top right) k_s ranging from 1 to 40 cm/d, other parameters from the best combination for Site 3. (bottom left) m ranging from 0.10 to 0.30, other parameters from the best combination for Site 3. (bottom right) ψ_s ranging from −6 to −30 cm, other parameters from the best combination for Site 3. Common parameters are those of climate (α, λ, and PET) and y_0, from the annual parameterizations for Site 3.

values of k_s (e.g., 1 cm/d and 10 cm/d) both the SWT and DWT regimes are present while for higher values of k_s (e.g., 20, 30 and 40 cm/d) only the SWT regime is present. An analogous situation can be noticed when varying ψ_s; in this case the pdf's relative to ψ_s = −6 and −12 cm show the presence of both the SWT and DWT regimes while the pdf's relative to the other three values of ψ_s tested are characterized by the presence of the only SWT regime.

[67] Starting from 20,000 different combinations of the four soil parameters, the "best" fit parameters for each site have been determined by filtering the results according to the best agreement between the model and the empirical pdf's in terms of their statistics (at both the annual and the seasonal levels). The most important comparison parameter between the model and the empirical pdf's is the central location, second the dispersion and, finally, the shape. Thus, the values of $\Delta\mu$, Δmd, $\Delta\sigma$ and $\Delta\gamma_1$ have been considered, assigning decreasing importance to each of them. The numerical procedure used to determinate for each site the 20 best combinations of soil parameters from the 20,000 combinations initially analyzed is described in detail in auxiliary material Text S1.[1]

[68] From the analysis of the best 20 combinations of soil parameters, one can derive some information useful to detect the set of soil parameters by which the model reproduce the empirical distributions more accurately, here referred to as the "best combination" for each site. Despite the use of relatively wide ranges for the four soil parameters at the beginning of the procedure (i.e., the ranges pointed out in section 3.4), the parameters relative to the resulting best 20 combinations converge in very narrow ranges. For example, most of the 20 best combinations of Site 1 show a value of ψ_s from −12.29 to −12.49 cm, n from 0.5 to 0.527 and m from 0.146 to 0.167. For Site 2, the ranges found are: k_s from 31.1 to 34.2 cm/d, n from 0.541 to 0.547 and ψ_s from −11.4 to −15.7 cm. For Site 3, one can notice that most of the 20 best combinations have m ranging from 0.168 to 0.188, k_s from 32 to 34.8 cm/d, n from 0.508 to 0.529 and ψ_s from −17.2 cm to −18 cm. Following the above considerations, for each site, the "best combination" of the soil parameters has been chosen among the 20 best combinations previously selected (Table 4).

4.2. Annual Analysis

[69] Figure 7 shows the results for the annual analysis obtained by using as soil parameters at each site the values reported in Table 4. It shows for the three different sites a

[1] Auxiliary material files are available in the HTML. doi:10.1029/2009WR008911.

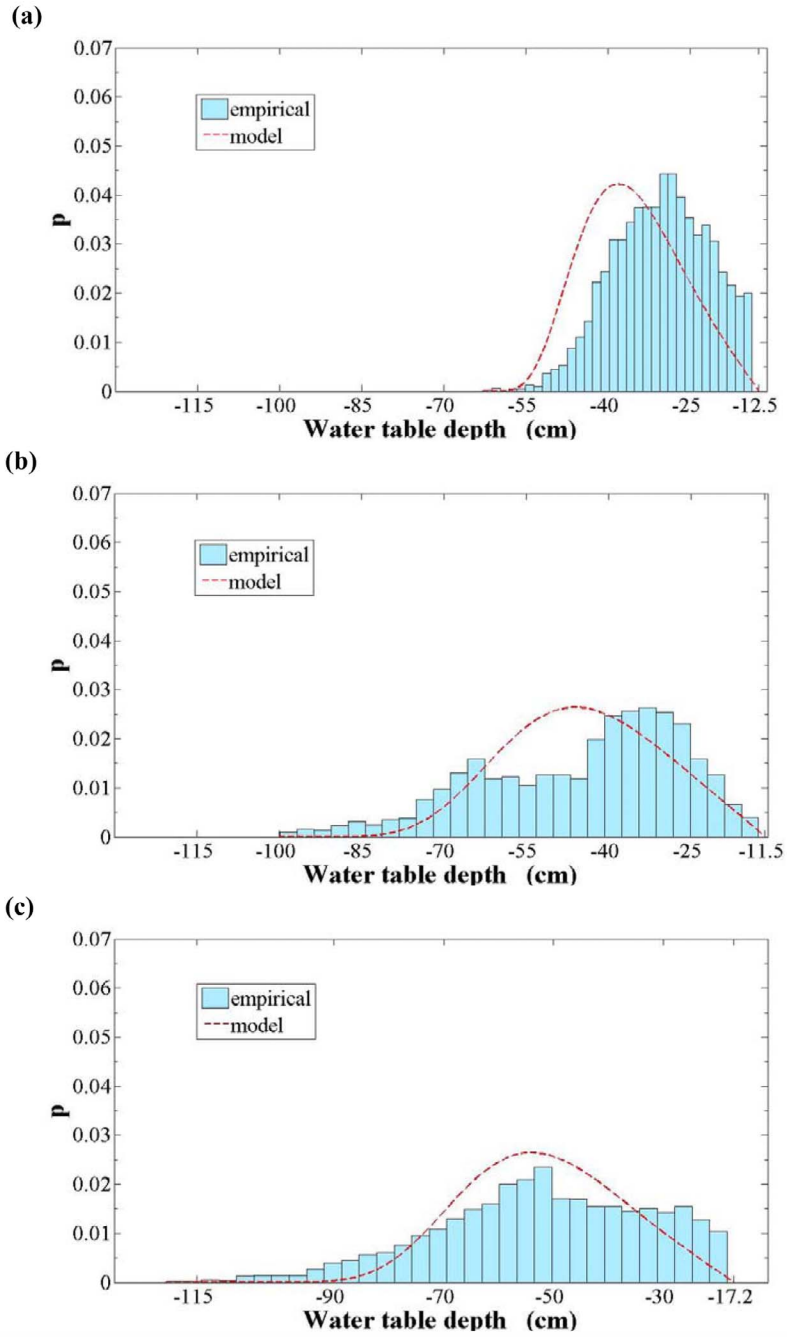

Figure 7. Annual analysis. Pdf's of the water table depth obtained from the model (using soil parameters corresponding to the best combinations in Table 4) compared to the empirical pdf's of the water table for (a) Site 1, (b) Site 2, and (c) Site 3.

qualitative comparison between the model pdf's of water table depth and the empirical ones at the annual scale. The water table depths are reported in cm with respect to the soil surface at each site.

[70] One notices that for Site 1 (Figure 7a) the mode of the model pdf is shifted toward a deeper groundwater position compared to the empirical pdf, while for the other two sites (Figures 7b and 7c) the modes of the model and empirical pdf's are very close. Table 5 provides a quantitative comparison showing that for Site 1 $\Delta\mu$ is about 5 cm, while for the other two sites the values of $\Delta\mu$ are around 1 mm. Regarding the dispersion, the values of σ relative to the model and the empirical pdf's are almost the same in the case of Site 1 while they differ more markedly for the other two sites ($\Delta\sigma$ is only 0.04 cm for Site 1, while it is around 4–5 cm for Site 2 and 3, Table 5).

[71] The shapes of the model and empirical pdf's are rather similar for Site 1 (Figure 7a), while they present some

Table 5. Statistics, at Both the Annual and the Seasonal Scale, Derived From the Empirical Pdf's (Observed) and the Model Pdf's (Modeled) Obtained by Using the Soil Parameters in Table 4[a]

	Observed				Modeled							
Site	μ (cm)	md (cm)	σ (cm)	γ_1	μ (cm)	md (cm)	σ (cm)	γ_1	$\Delta\mu$ (cm)	Δmd (cm)	$\Delta\sigma$ (cm)	$\Delta\gamma_1$
					Annual							
1	−30.3	−29.8	8.7	−0.22	−35.6	−36.7	8.8	0.20	5.4	6.9	0.0	0.42
2	−44.6	−40.1	18.2	−0.62	−44.7	−45.3	13.8	−0.02	0.1	5.2	4.4	0.59
3	−52.1	−51.6	19.5	−0.43	−52.1	−52.9	14.0	0.03	0.1	1.3	5.6	0.46
					Dry Season							
1	−34.6	−34.7	7.9	0.03	−40.0	−41.5	8.6	0.51	5.4	6.8	0.8	0.47
2	−54.8	−56.3	16.2	−0.07	−68.3	−70.5	12.2	0.82	13.5	14.2	4.0	0.89
3	−61.3	−61.4	18.5	−0.10	−83.2	−85.3	12.2	0.82	22.0	23.9	6.3	0.92
					Wet Season							
1	−25.4	−25.2	6.9	−0.37	−24.9	−25.2	5.7	−0.21	0.5	0.0	1.0	0.17
2	−34.1	−31.9	13.7	−1.94	−34.0	−33.6	11.2	−0.41	0.1	1.7	2.5	1.53
3	−41.0	−40.3	14.3	−0.72	−37.1	−37.0	9.6	−0.37	3.8	3.4	4.7	0.35

[a]Mean, μ; median, md; standard deviation, σ; skewness, γ_1. $\Delta\mu = |\mu^{mod} - \mu^{obs}|$ in cm; $\Delta md = |md^{mod} - md^{obs}|$ in cm; $\Delta\sigma = |\sigma^{mod} - \sigma^{obs}|$ in cm; $\Delta\gamma_1 = |\gamma_1^{mod} - \gamma_1^{obs}|$.

differences at Site 2, where the empirical pdf appears bimodal (Figure 7b). From Table 1, one can note that the difference between the mean seasonal depths of the water table during the dry and the wet season at Site 2 is almost two times that of Site 1. This could be physically explained by the presence of a nearby canal, where the mean water levels during the wet and the dry seasons are at consistently different positions (see Table 3). This fact leads to different lateral flow contributions during the two seasons that, obviously, affect the water table positions at the seasonal scale, and, as a consequence, also at the annual scale. From the analysis of the historical data of water table for Site 2 (section 2.3) one can note that after removing the seasonality from the original series, the "detrended" series of water levels still presents a strong signal in the ACF (Figure 4b, middle) due to the influence of the nearby canal on the water table dynamics. This confirms that the canals subject to human management may considerably impact the natural dynamics of the water table. Analogous considerations could be applied for Site 3, whose nearest water body is also a canal. In fact, the empirical pdf of Site 3 (Figure 7c) also shows a weak impact of seasonality, with a slight bimodal shape, even if this behavior is much less marked than in the case of Site 2. The fact that the empirical pdf's of Site 2 and Site 3 show bimodal features may also result from their different soil properties (such as the hydraulic conductivity) with respect to those relative to Site 1. In fact, the saturated hydraulic conductivities for Sites 2 and 3, according to the results of the procedure discussed above (section 4.1) is almost three times that relative to Site 1 (see Table 4) and this would makes the water table dynamics faster at these two sites, thus emphasizing the effects of the seasonal climatic variability on the water table fluctuations.

[72] The model, working at the annual scale, considers a water level in the external canals to be constant and equal to the annual mean. For this reason, it is not able to take into account the difference in the seasonal contributions of the lateral flow. Moreover, the use of climatic parameters at the annual scale leads the model to reduce the effect of the seasonal climatic variability.

[73] In Table 5, the values of the statistics relative to the observed series and those arising from the model pdf's are also shown. It can be noted that, at the annual scale and for all the sites, the model mean and medians values are always slightly lower than those observed (i.e., the mean and median positions of the water table derived from the model are deeper than that observed). The values of the standard deviation from the model are rather similar to those observed, with differences always lower than 5.5 cm, even if there is some consistent underestimation. This means that the model underestimates the variability of the observed process (except for Site 1, where the annual model standard deviation is almost the same as the observed one). From Table 5 it can be also noted that, at the annual scale, the empirical distributions are rather skewed to the left (negatively skewed) for all the three site (especially at Site 2) while the model pdf's for Site 2 and 3 are rather symmetric, and only at Site 1 a slight positive asymmetry can be noticed.

4.3. Seasonal Analysis

[74] As shown in Table 2, the wet season is characterized by more intensive and frequent rainfall events, with a total amount of precipitation near three times the values of the dry season. Thus a higher amount of water infiltrates the soil but, at the same time, there is a higher rate of evapotranspiration. The resulting water table is shallower during the wet season (see Table 1) and all the observed periods of submergence occur during this season (see Figure 3). Moreover, during the dry season, the water table fluctuates through a wider range of depths than during the wet season because of the prolonged dry period from December to May.

[75] Table 5 reports some of the quantitative results of the seasonal analysis, while Figure 8 shows a qualitative comparison between the seasonal pdf's resulting from the model and the empirical data.

[76] The model results at a seasonal level are not as accurate as at the annual level, especially for the dry season. This is mainly evident at Sites 2 and 3 (Figures 8b and 8c), while the model performs better at Site 1 (Figure 8a). For all the sites, the model pdf's of water table shift toward shal-

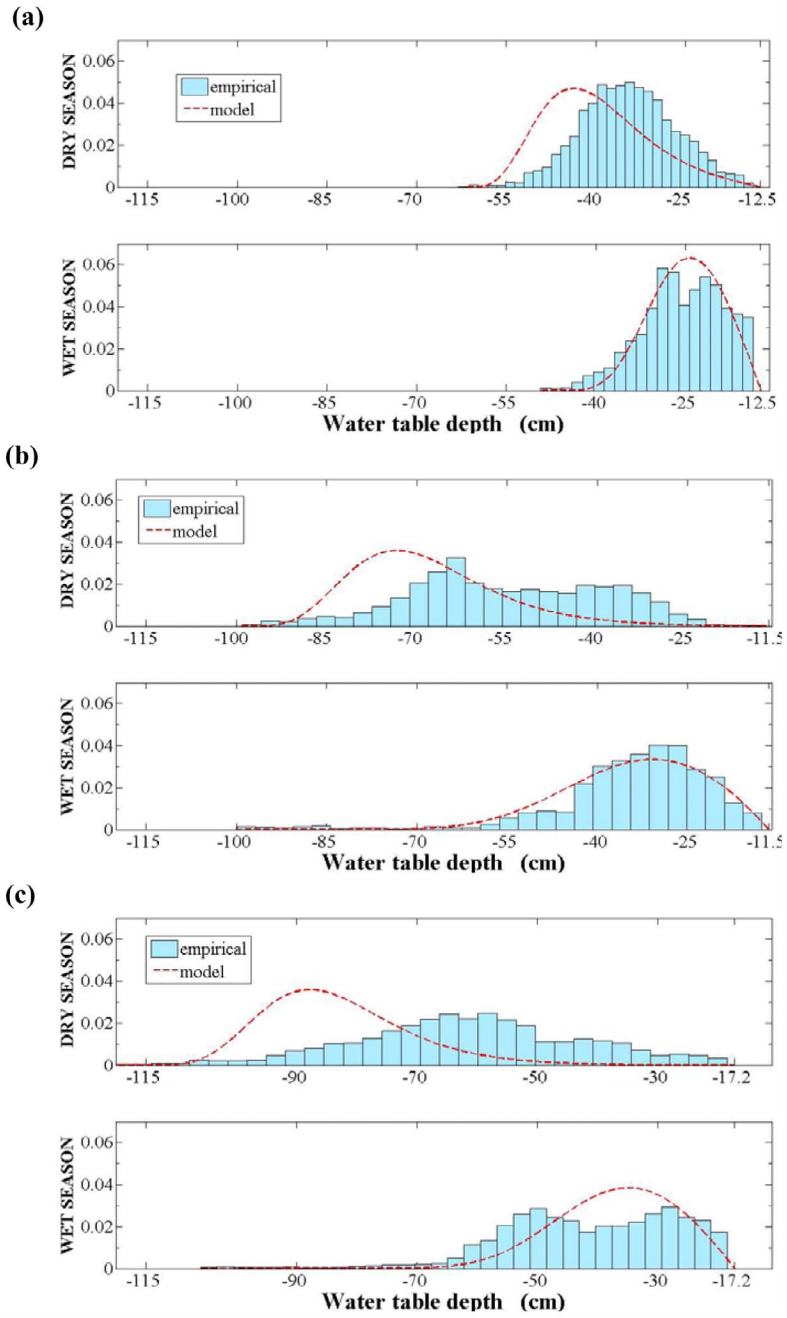

Figure 8. Seasonal analysis. Pdf's of the water table depth obtained from the model (using soil parameters corresponding to the best combinations in Table 4) compared to the empirical ones for (a) Site 1, (b) Site 2, and (c) Site 3. For each site are shown (top) the dry season (from December to May) and (bottom) the wet season (from June to November).

lower values during the wet season and toward deeper values during the dry season. This behavior is probably due to the dependency of the water table position to the initial condition at the beginning of each season, rather than to the model parameters for the season itself. The initial condition is expected to play an important role, especially when the differences between the two seasons are marked, and it cannot be accounted for by the model which represents only a steady state statistical condition.

[77] The persistence of a shallow water table at the end of the wet season and the relatively slow dynamics of the water table, influence the water table depth over almost the entire dry season. Similarly, the initial condition at the beginning of the wet season influences the water table position during the period from June to November but, because the rainfall events are more frequent and intense, it is likely that a steady condition is reached earlier than for the case of the dry season. This explains the fact that the model performs better for the wet season. Table 5 shows that during the dry

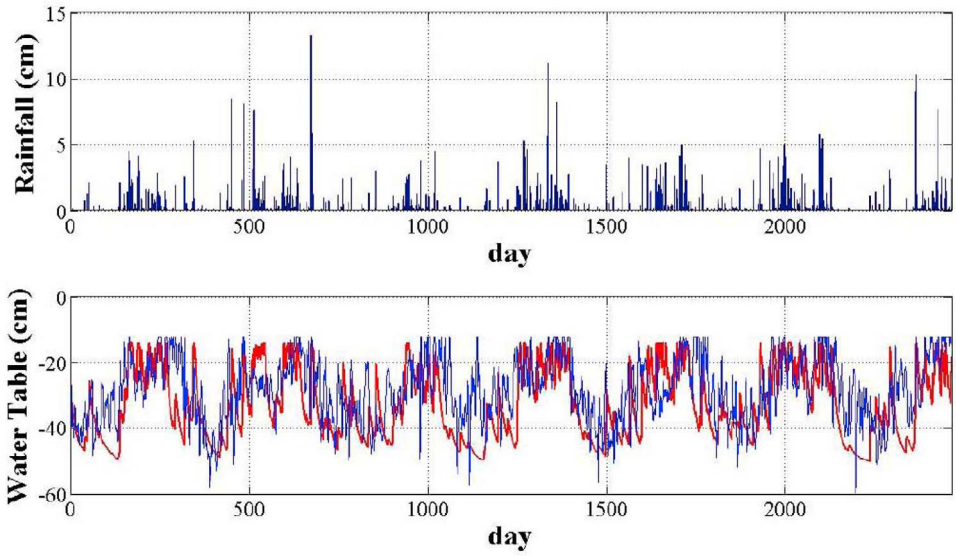

Figure 9. (top) Daily rainfall series. (bottom) Comparison between the observed daily water table time series (blue) and the synthetic model generated series (red) obtained by numerical integration of equation (2). Site 1 with observation period from 1 January 2002 to 30 September 2008.

season the values of mean and median derived from the model are lower (i.e., deeper positions) than those derived from the empirical pdf's, especially for Sites 2 and 3 (the differences $\Delta\mu$ and Δmd are on the order of 6 cm for Site 1, 14 cm for Site 2 and 22 cm for Site 3). The central location of the model pdf's relative to the wet season is very close to that of the correspondent empirical pdf's for Sites 1 and 2, while for Site 3 the model mean and median are about 3.5 cm higher than the observed ones. Another reason that, in a minor way, could affect the model accuracy in the seasonal reproduction of the water table dynamics during the dry season is that when the water flow is oriented upward, the soil at the three sites may have an upward hydraulic conductivity higher than the one downward (*Myers*, 1999). Such behavior which may enhance the ability of wetlands to maintain a shallow water table is not represented in the analytical model.

[78] Although in the seasonal analysis the model takes into account the different seasonal contributions of the lateral flow, by considering two different water levels into the canals (one for each season, that is equal to the mean seasonal position), the presence of canals as external water bodies is also responsible for discrepancies between the model and the empirical pdf's of the water table. As in the case of the annual analysis, the water surface of the external water body has been considered constant in time for each season, while, in reality, the water levels in the canals are subjected to daily fluctuations which may increase the variability of water table position, and that the model is not able to consider. As can be observed from Table 5, the variability of the process is better reproduced at Site 1 than in the other two sites. In fact, the values of standard deviation relative to the model pdf's, for both the dry and wet season, are rather close to those obtained from the observed series (with $\Delta\sigma$ on the order of 1 cm), while for the other two sites the values of $\Delta\sigma$ are on the order of 2.5–4.5 cm for the wet season and 4–6 cm for the dry season (with the higher values referring to Site 3), with the model underestimating the variability of the observed process.

4.4. Comparison Between Observed and Synthetic Water Table Time Series

[79] Many species find their niche based on not only in the frequency at which a certain depth is exceeded, but also in the duration of high saturation levels (i.e., how long a plant can endure oxygen stress). Thus it is interesting to study the autocorrelation and power spectrum functions of the synthetic series produced by the model and how they compare with the observed ones. Besides their own intrinsic interest these functions also control the crossing properties of the processes.

[80] The autocorrelation and power spectrum of simulated water table positions have been studied through the numerical integration of equation (2) with constant values of PET and y_0 as it is assumed in the model (following the same approach as that of *Pumo et al.* [2008]). All the available rainfall data (e.g., from 1/1/2002 to 9/30/2008) were used as input to the model using the "best" combination of soil and vegetation parameters for Site 1 (see Table 4).

[81] The resulting series of daily water table positions is shown in Figure 9 which also shows the historical data at Site 1. These two series have been also compared through their autocorrelation and power spectral characteristics. The comparison is shown in Figure 10 for both, the original series as well as their deseasonalized versions (in order to remove the seasonality, the same procedure as in section 2.3 has been used).

[82] From Figures 9 and 10 one can observe that although there are differences in the second order properties between the data and the synthetic series, they are similar in their general structure despite the necessary simplifications incorporated in the model. Note that the ACFs and the PSFs shown in Figure 10 for the observed series (blue lines) are slightly different from those shown in Figure 4a; this is

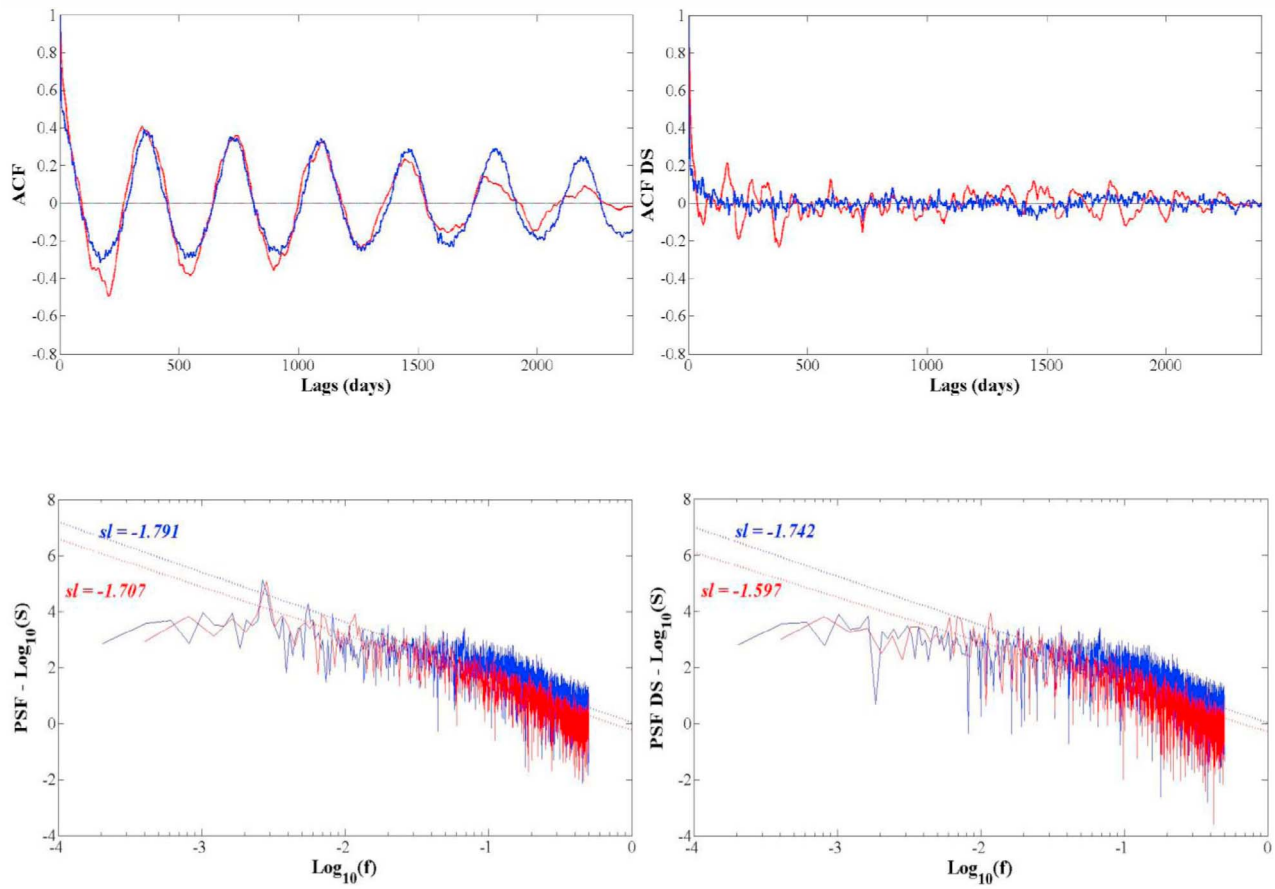

Figure 10. (top left) Comparison between the autocorrelation functions (ACF) for the original observed water table series (blue) and the synthetic series (red). (top right) The ACFs of the detrended series after the removal of the seasonal cycle (ACF DS) for the observed (blue) and the synthetic (red) series. (bottom left) Comparison between the power spectra functions (PSF) of the original observed (blue) and synthetic (red) series. (bottom right) Comparison between the PSFs for the detrended series (PSF DS) observed (blue) and synthetic (red). The synthetic series have been obtained by numerical integration of equation (2). Site 1 with observation period from 1 January 2002 to 30 September 2008.

because the time span considered for the comparison with the synthetic series (i.e., from 1/1/2002 to 9/30/2008) is shorter than that used previously (i.e., from 10/2/95 to 1/26/2009, that is the entire series available). Although similar in their general structure it is observed that the synthetic series produced by the model are more locally noisy than the observed data.

5. Conclusions

[83] Considering the increasing attention devoted in recent years to wetlands and groundwater-dependent ecosystems, it is becoming increasingly important to develop and test quantitative models for the analysis of such ecosystems. A recent ecohydrological model proposed by *Laio et al.* [2009] provides a probabilistic description of the water table depths and fluctuations in groundwater-dependent ecosystems. The model is based on a simple process-based soil water balance and provides an analytical description of the statistical structure of the water table levels. Since this model has never been applied to real cases, this paper represents a first test of such a model with field data.

[84] The model has been applied to three sites in the Florida Everglades using both the annual and seasonal parameterizations. The resulting pdf's of water table depths have been compared to those resulting from the daily historical series recorded at each site. A sensitivity analysis of the model to some parameters has been also performed, showing how the model results are only slightly dependent on the vegetation parameter b (i.e., average rooting depth), while they are strongly dependent on the soil parameters, and in particular, on the bubbling pressure head (ψ_s) and saturated hydraulic conductivity (k_s).

[85] The annual analysis has shown the capability of the model to reproduce the observed distribution, using mean annual values of rainfall depth and frequency, evapotranspiration and water surface position of the nearest water body as input parameters. Since Sites 2 and 3 are characterized by the presence of a nearby canal, where the water levels during the dry season are at consistently different position from those during the wet season, the empirical pdf's of the water table present a bimodal shape that the model is unable to reproduce at the annual scale. Using the seasonal parameterization, the model still reproduces the observed pdf in Site 1 quite well. For the other two sites, the seasonal pdf's are

strongly affected by the initial position of the water table at the beginning of each season and the model is less accurately on the reproduction of the observed pdf's. In particular, during the dry season, the model pdf's are shifted toward deeper values, while the pdf's of the wet season are shifted toward shallower water table values. This effect is much more evident during the dry season, when reaching a steady state condition requires more time than that required during the wet season.

[86] The model results, in both the annual and seasonal analysis, are affected by the assumption of an external water surface constant in time, while specially the water level in the canals are subjected to strong daily/seasonal fluctuations which may increase the variability of water table positions.

[87] The discrepancies between the observed values and the model results may be explained by the soil parameters chosen for the sites under consideration which have been evaluated after an optimization procedure based on the similarity between the model and observed pdf's statistics, rather than through field or laboratory analyses. Furthermore, the model assumes the soil is homogeneous and isotropic while organic soils, such as those of the Everglades, are known to have an anisotropic and hysteretic behavior. In addition to this, the rainfall and evapotranspiration parameters are estimated with time series shorter than those of the water table depths, and might be not fully representative of the climatic conditions occurring throughout time.

[88] In conclusion, the model at the annual level has shown an acceptable ability to reproduce the probabilistic description of the water table dynamics for groundwater-dependent ecosystems having limited hydroperiods. The study of frequently submerged sites, such as it is commonly found in the Everglades, requires the explicit consideration of the dynamics of water levels above the soil surface. This is the most important direction of ongoing research.

[89] **Acknowledgments.** This work was funded by the National Aeronautics and Space Administration NASA Cooperative Agreement NNX08BA43A (WaterSCAPES: Science of Coupled Aquatic Processes in Ecosystems from Space) and the National Science Foundation under grant 0642517 (Co-organization of River Basin Geomorphology and Vegetation). The authors gratefully acknowledge the help of the U.S. Geological Survey (USGS) and the Everglades Depth Estimation Network (EDEN). Some of the data sets were provided by the Florida Coastal Everglades Long-Term Ecological Research (LTER) Program.

References

Bartholomeus, R. P., M. Witte, P. M. van Bodegom, J. C. van Dam, and R. Aerts (2008), Critical soil conditions for oxygen stress to plant roots: Substituting the Feddes-function by a process-based model, *J. Hydrol.*, *360*(1–4), 147–165, doi:10.1016/j.jhydrol.2008.07.029.

Berendrecht, W. L., A. W. Heemink, F. C. van Geer, and J. C. Gehrels (2004), State-space modeling of water table fluctuations in switching regimes, *J. Hydrol.*, *292*(1–4), 249–261, doi:10.1016/j.jhydrol.2004.01.001.

Bierkens, M. F. P. (1998), Modeling water table fluctuations by means of a stochastic differential equation, *Water Resour. Res.*, *34*(10), 2485–2499, doi:10.1029/98WR02298.

Boelter, D. H. (1965), Hydraulic conductivity of peats, *Soil Sci.*, *100*(4), 227–231, doi:10.1097/00010694-196510000-00001.

Boggie, R. (1970), Moisture characteristics of some peat-sand mixtures, *Sci. Horticult.*, *22*, 87–91.

Botter, G., A. Porporato, I. Rodriguez-Iturbe, and A. Rinaldo (2007), Basin-scale soil moisture dynamics and the probabilistic characterization of carrier hydrologic flows: Slow, leaching-prone components of the hydrologic response, *Water Resour. Res.*, *43*, W02417, doi:10.1029/2006WR005043.

Brinson, M. M. (1993), A hydrogeomorphic classification for wetlands, *Tech. Rep. WRP-DE-4*, Wetlands Res. Program, U.S. Army Corps of Eng., Vicksburg, Miss., August.

Brolsma, R. J., and M. F. P. Bierkens (2007), Groundwater–soil water–vegetation dynamics in a temperate forest ecosystem along a slope, *Water Resour. Res.*, *43*, W01414, doi:10.1029/2005WR004696.

Brooks, R. H., and A. T. Corey (1964), *Hydraulic Properties of Porous Media*, *Hydrol. 386 Pap. 3*, Colo. State Univ., Fort Collins.

Chason, D. B., and D. I. Siegel (1986), Hydraulic conductivity and related physical properties of Peat, Lost River Peatland, northern Minnesota, *Soil Sci.*, *142*, 91–99, doi:10.1097/00010694-198608000-00005.

Costanza, R., O. Perez-Marqueo, M. L. Martinez, P. Sutton, S. J. Anderson, and K. Mulder (2008), The value of coastal wetlands for hurricane protection, *Ambio*, *37*(4), 241–248.

Dacey, J. W. H., and B. H. Howes (1984), Water uptake by roots controls water table movement and sediment oxidation in short *Spartina* marsh, *Science*, *224*, 487–489, doi:10.1126/science.224.4648.487.

Dai, T. S., and J. H. Sparling (1973), Measurement of hydraulic conductivity of peats, *Can. J. Soil Sci.*, *53*, 21–26, doi:10.4141/cjss73-003.

D'Odorico, P., and A. Porporato (2004), Preferential states in soil moisture and climate dynamics, *Proc. Natl. Acad. Sci. U. S. A.*, *101*(24), 8848–8851, doi:10.1073/pnas.0401428101.

D'Odorico, P., and A. Porporato (2006), *Dryland Ecohydrology*, Springer, New York, doi:10.1007/1-4020-4260-4.

Dubé, S., A. P. Plamondon, and R. L. Rothwell (1995), Watering up after clear-cutting on forested wetlands of the St. Lawrence lowland, *Water Resour. Res.*, *31*(7), 1741–1750, doi:10.1029/95WR00427.

Eamus, D. (2009), *Identifying Groundwater Dependent Ecosystems*, Univ. of Technol., Land and Water Australia, Sydney, Australia.

Feddes, R. A., P. Kabat, P. J. T. Vanbakel, J. J. B. Broswijk, and J. Albertsma (1988), Modeling soil-water dynamics in the unsaturated zone—State of the art, *J. Hydrol.*, *100*(1–3), 69–111, doi:10.1016/0022-1694(88)90182-5.

Gilvear, D. J., J. H. Tellam, J. W. Lloyd, and D. N. Lerner (1989), *The Hydrodynamics of East Anglian Fen Systems*, Hydrogeol. Res. Group, School of Earth Sci., Univ. of Birmingham, Edgbaston, U. K.

Guswa, A. J. (2005), Soil-moisture limits on plant uptake: An upscaled relationship for water-limited ecosystems, *Adv. Water Resour.*, *28*(6), 543–552, doi:10.1016/j.advwatres.2004.08.016.

Guswa, A. J. (2008), The influence of climate on root depth: A carbon cost-benefit analysis, *Water Resour. Res.*, *44*, W02427, doi:10.1029/2007WR006384.

Hoag, R. S., and J. S. Price (1995), A field-scale, natural gradient solute transport experiment in peat at a Newfoundland blanket bog, *J. Hydrol.*, *172*, 171–184, doi:10.1016/0022-1694(95)02696-M.

Holden, J., and T. P. Burt (2003), Hydrological studies on blanket peat: The significance of the acrotelm-catotelm model, *J. Ecol.*, *91*, 86–102, doi:10.1046/j.1365-2745.2003.00748.x.

Ingram, H. A. P. (1967), Problems of hydrology and plant distribution in mires, *J. Ecol.*, *55*(3), 711–724, doi:10.2307/2258420.

Katimon, A., and L. Melling (2007), Moisture retention curve of tropical sapric and hemic peat, *Malaysian J. Civ. Eng.*, *19*(1), 84–90.

Kim, C. P., G. D. Salvucci, and D. Entekhabi (1999), Groundwater-surface water interaction and the climatic spatial patterns of hillslope hydrological response, *Hydrol. Earth Syst. Sci.*, *3*, 375–384, doi:10.5194/hess-3-375-1999.

Kozlowski, T. T. (1984), Responses of woody plants to flooding, in *Flooding and Plant Growth*, edited by T. T. Kozlowski, pp. 129–163, Elsevier, New York.

Laio, F., A. Porporato, L. Ridolfi, and I. Rodriguez-Iturbe (2001), Plants in water-controlled ecosystems: Active role in hydrologic processes and response to water stress II. Probabilistic soil moisture dynamics, *Adv. Water Resour.*, *24*, 707–723, doi:10.1016/S0309-1708(01)00005-7.

Laio, F. (2006), A vertically extended stochastic model of soil moisture in the root zone, *Water Resour. Res.*, *42*, W02406, doi:10.1029/2005WR004502.

Laio, F., P. D'Odorico, and L. Ridolfi (2006), An analytical model to relate the vertical root distribution to climate and soil proprieties, *Geophys. Res. Lett.*, *33*, L18401, doi:10.1029/2006GL027331.

Laio, F., S. Tamea, L. Ridolfi, P. D'Odorico, and I. Rodriguez-Iturbe (2009), Ecohydrology of groundwater-dependent ecosystems: 1. Stochastic water table dynamics, *Water Resour. Res.*, *45*, W05419, doi:10.1029/2008WR007292.

Little, E. L., Jr. (1983), *Common Fuelwood Crops: A Handbook for Their Identification*, McClain, Parsons, W. Va.

Lodge, T. E. (2004), *The Everglades Handbook: Understanding the Ecosystem*, 2nd ed., CRC Press, Boca Raton, Fla.

Mitsch, W. J., and J. G. Gosselink (2007), *Wetlands*, 4th ed., John Wiley, Hoboken, N. J.

Mitsch, W. J., J. G. Gosselink, L. Zhang, and C. J. Anderson (2009), *Wetlands Ecosystems*, John Wiley, New York.

Myers, R. D. (1999), Hydraulic proprieties of South Florida wetland peats, thesis, Univ. of Florida, Gainesville.

Morel-Seytoux, H. J., P. D. Meyer, M. Nachabe, J. Touma, M. T. van Genuchten, and R. J. Lenhard (1996), Parameter equivalence for the Brooks-Corey and van Genuchten soil characteristics: Preserving the effective capillary drive, *Water Resour. Res.*, *32*(5), 1251–1258, doi:10.1029/96WR00069.

Naasz, R., J. C. Michel, and S. Charpentier (2005), Measuring hysteretic hydraulic properties of peat and pine bark using a transient method, *Soil Sci. Soc. Am. J.*, *69*, 13–22, doi:10.2136/sssaj2005.0013.

Naiman, R. J., H. Decamps, and M. E. McClain (2005), *Riparia*, Elsevier, New York.

Naumburg, E., R. Mata-Gonzalez, R. G. Hunter, T. McLendon, and D. W. Martin (2005), Phreatophytic vegetation and groundwater fluctuations: A review of current research and application of ecosystem response modeling with an emphasis on great basin vegetation, *Environ. Manage. N. Y.*, *35*(6), 726–740, doi:10.1007/s00267-004-0194-7.

Novitzki, R. P. (1979), Hydrologic characteristics of Wisconsin's wetlands and their influence on floods, stream flow, and sediment, in *Wetland Functions and Values: The State of Our Understanding*, edited by P. E. Greeson, J. R. Clark, and J. E. Clark, pp. 377–388, Am. Water Resour. Assoc., Minneapolis, Minn.

O'Brien, A. L. (1977), Hydrology of two small wetland basins in eastern Massachusetts, *Water Resour. Bull.*, *13*(2), 325–340.

Porporato, A., and P. D'Odorico (2004), Phase transitions driven by state-dependent Poisson noise, *Phys. Rev. Lett.*, *92*(11), 110601, doi:10.1103/PhysRevLett.92.110601.

Porporato, A., F. Laio, L. Ridolfi, and I. Rodriguez-Iturbe (2001), Plants in water-controlled ecosystems: Active role in hydrologic processes and response to water stress III. Vegetation water stress, *Adv. Water Resour.*, *24*, 725–744, doi:10.1016/S0309-1708(01)00006-9.

Pumo, D., F. Viola, and L. V. Noto (2008), Ecohydrology in Mediterranean areas: A numerical model to describe growing season out of phase with precipitations, *Hydrol. Earth Syst. Sci.*, *12*, 303–316, doi:10.5194/hess-12-303-2008.

Ramsar Convention Bureau (1996), Wetlands and biological diversity: Cooperation between the convention of wetlands of international importance especially as waterfowl habitat (Ramsar, Iran, 1971) and the convention on biological diversity, *Doc. UNEP/CBD/COP/3/Inf.21*, Nairobi.

Rawls, W. J., and D. L. Brakensiek (1989), Estimation of soil water retention and hydraulic proprieties, in *Unsaturated Flow in Hydrological Modeling*, edited by H. J. Morel-Seytoux, pp. 275–300, Kluwer Acad., Dordrecht, Netherlands.

Renken, R. A., J. Dixon, J. Koehmstedt, S. Ishman, A. C. Lietz, R. L. Marella, P. Telis, J. Rogers, and S. Memberg (2005), *Impact of Anthropogenic Development on Coastal Ground-Water Hydrology in Southeastern Florida, 1900–2000*, *Circ. 1275*, Greater Everglades Priority Ecosyst. Sci. Program, U.S. Geol. Surv., Ft. Lauderdale, Fla.

Ridolfi, L., P. D'Odorico, F. Laio, S. Tamea, and I. Rodriguez-Iturbe (2008), Coupled stochastic dynamics of water table and soil moisture in bare soil condition, *Water Resour. Res.*, *44*, W01435, doi:10.1029/2007WR006707.

Rizzuti, A. M., A. D. Cohen, and E. M. Stack (2004), Using hydraulic conductivity and micropetrography to assess water flow through peat-containing wetlands, *Int. J. Coal Geol.*, *60*, 1–16, doi:10.1016/j.coal.2004.03.003.

Rodriguez-Iturbe, I., and A. Porporato (2004), *Ecohydrology of Water-Controlled Ecosystem: Soil Moisture and Plant Dynamics*, Cambridge Univ. Press, Cambridge, U. K.

Rodriguez-Iturbe, I., A. Porporato, L. Ridolfi, V. Isham, and D. R. Cox (1999), Probabilistic modelling of water balance at a point: The role of climate, soil and vegetation, *Proc. R. Soc. London, Ser. A*, *455*, 3789–3805, doi:10.1098/rspa.1999.0477.

Rodriguez-Iturbe, I., P. D'Odorico, F. Laio, L. Ridolfi, and S. Tamea (2007), Challenges in humid land ecohydrology: Interactions of water table and unsaturated zone with climate, soil, and vegetation, *Water Resour. Res.*, *43*, W09301, doi:10.1029/2007WR006073.

Rosa, E., and M. Larocque (2008), Investigating peat hydrological proprieties using field and laboratory methods: Application to the Lanoraie peatland complex, *Hydrol. Processes*, *22*, 1866–1875, doi:10.1002/hyp.6771.

Roy, V., J.-C. Ruel, and A. P. Plamondon (2000), Establishment, growth and survival of natural regeneration after clearcutting and drainage on forested wetlands, *For. Ecol. Manage.*, *129*, 253–267, doi:10.1016/S0378-1127(99)00170-X.

Salvucci, G. D., and D. Entekhabi (1994), Equivalent steady soil moisture profile and the time compression approximation in water balance modeling, *Water Resour. Res.*, *30*, 2737–2749, doi:10.1029/94WR00948.

Salvucci, G. D., and D. Entekhabi (1995), Hillslope and climatic controls on hydrologic fluxes, *Water Resour. Res.*, *31*(7), 1725–1739, doi:10.1029/95WR00057.

Schenk, H. J. (2005), Vertical vegetation structure below ground: Scaling from root to globe, *Prog. Bot.*, *66*, 341–373, doi:10.1007/3-540-27043-4_14.

Schenk, H. J., and R. B. Jackson (2002), The global biogeography of roots, *Ecol. Monogr.*, *72*(3), 311–328, doi:10.1890/0012-9615(2002)072[0311:TGBOR]2.0.CO;2.

Srinivas, H., and Y. Nakagawa (2008), Environmental implications for disaster preparedness: Lessons learnt from the Indian Ocean Tsunami, *J. Environ. Manage.*, *89*(1), 4–13, doi:10.1016/j.jenvman.2007.01.054.

Sturges, D. L. (1968), Hydrologic properties of peat from a Wyoming mountain bog, *Soil Sci.*, *106*, 262–264, doi:10.1097/00010694-196810000-00003.

Tamea, S., F. Laio, L. Ridolfi, P. D'Odorico, and I. Rodríguez-Iturbe (2009), Ecohydrology of groundwater-dependent ecosystems: 2. Stochastic soil moisture dynamics, *Water Resour. Res.*, *45*, W05420, doi:10.1029/2008WR007293.

Vartapetian, B. B., and M. B. Jackson (1997), Plant adaptation to anaerobic stress, *Ann. Bot.*, *79*(A), 3–20.

Walczak, R., E. Rovdan, and B. Witkowska-Walczak (2002), Water retention characteristics of peat and sand mixtures, *Int. Agrophys.*, *16*, 161–165.

Weaver, H. A., and W. H. Speir (1960), Applying basic soil water data to water control problems in Everglades peaty muck, *41-40*, 15 pp., U.S. Agricult. Res. Serv., Washington, D. C.

Wright, J. M., and J. C. Chambers (2002), Restoring riparian meadows currently dominated by Artemisia using alternative state concepts—Aboveground response, *Appl. Veg. Sci.*, *5*, 237–246, doi:10.1658/1402-2001(2002)005[0237:RRMCDB]2.0.CO;2.

Yates, S. A. (1974), An autecological study of sawgrass, Cladium jamaicense, in southern Florida, thesis, 117 pp., Univ. of Miami, Coral Gables, Fla.

Yeh, P. J. F., and E. A. B. Eltahir (2005), Representation of water table dynamics in a land surface scheme. part I: Model development, *J. Clim.*, *18*(12), 1861–1880, doi:10.1175/JCLI3330.1.

F. Miralles-Wilhem, Department of Civil and Environmental Engineering, Florida International University, Miami, FL 33174, USA.

L. V. Noto and D. Pumo, Dipartimento di Ingegneria Idraulica ed Applicazioni Ambientali, Università degli Studi di Palermo, Viale delle Scienze, I-90128 Palermo, Italy. (pumo@unipa.it)

I. Rodriguez-Iturbe, Department of Civil and Environmental Engineering, Princeton University, E-220 Engineering Quad, Princeton, NJ 08544, USA.

S. Tamea, Dipartimento di Idraulica, Trasporti ed Infrastrutture Civili, Politecnico di Torino, Corso Duca degli Abruzzi 24, I-10129 Torino, Italy.